Density of methanolic alkali halide salt solutions by experiment and molecular simulation

Steffen Reiser, Martin Horsch,* and Hans Hasse

Laboratory of Engineering Thermodynamics, University of Kaiserslautern, 67653 Kaiserslautern, Germany

E-mail: martin.horsch@mv.uni-kl.de

Abstract

The density of methanolic alkali halide salt solutions is studied experimentally at 298.15 K, 308.15 K and 318.15 K at 1 bar for solutions containing all soluble combinations of alkali cations (Li^+, Na^+, K^+, Rb^+, Cs^+) with halide anions (F^-, Cl^-, Br^-, I^-) at concentrations up to 0.05 mol/mol or 90 % of the solubility limit. The density of the electrolyte solutions is also determined by molecular simulation in the same temperature and composition range. The used force fields of the ions were adjusted in previous work to properties of aqueous solutions and the solvent methanol to pure component properties. The force fields are of the Lennard-Jones (LJ) plus point charge type in case of the ions and of the LJ plus partial charges type in case of the solvent. For the present molecular simulations, no further adjustment of the force fields is carried out. The mixed interactions between the ions and methanol are predicted by the Lorentz-Berthelot combining rules. The predictions of the reduced density by molecular simulation are found to be in very good agreement with the experimental data. Furthermore, the radial distribution function of methanol around the ions, the solvation number and the residence time of methanol molecules in the first solvation shell, the self-diffusion coefficient

*To whom correspondence should be addressed

of the ions and the electric conductivity is systematically studied by molecular simulation and compared to experimental literature data where available.

Keywords: methanolic electrolyte solutions, alkali halide salts, density measurements, molecular simulation

1. Introduction

Methanolic electrolyte solutions play an important role in many industrial applications, especially in the field of the electrochemistry.[1,2] Their thermodynamic properties can be described by phenomenological models.[3] However, these models have many adjustable parameters[3,4] and are limited to the range of the experimental data they were adjusted to. In addition it is known that such phenomenological models are not transferable to other solvents.[3–5]

Molecular simulations with classical force fields go far beyond these methods. The thermodynamic properties of different combinations of salts with solvents can be estimated at arbitrary conditions. Furthermore, these simulations also provide a detailed insight into the structure and the processes in the solution on the molecular level. However, this requires accurate force fields both for the ions and the solvents. The density, which is closely related to the intermolecular distances, is vital for the validation of any kind of force field. The prediction of thermodynamic properties of methanolic alkali halide salt solutions by molecular simulation is influenced by the accuracy of the used force fields both of the ions and methanol.

In the recent years, many different force fields for the alkali cations and halide anions have been developed.[6–19] Although different parameterization strategies with different objectives were applied, these force fields have in common that they were adjusted to data of aqueous electrolyte solutions, e.g. to the free energy,[15,16,18] the activity[17,19] as well as the density of the solutions.[13] The strategies and the capabilities of the resulting force fields in aqueous electrolyte solutions are discussed in more detail by Reiser et al.[20] and Moucka et al.[21] In recent work of our group, force fields for all alkali cations and halide anions were developed.[20,22] These ion force fields consist

of one Lennard-Jones (LJ) site and a concentric point charge with the magnitude of ±1 e. The LJ size parameters were adjusted in a global fit to reduced densities of all aqueous alkali halide salt solutions at 293.15 K and 1 bar. The LJ energy parameter, which has only a minor influence on the density,[22] was adjusted to the self-diffusion coefficient of the ions in aqueous solution in combination with the position of the first maximum of the radial distribution function (RDF) of water around the ions at 293.15 K and 298.15 K, respectively, and 1 bar. The reduced density, which is defined as the density of the electrolyte solution divided by the density of the pure solvent, was considered as an objective for the optimization rather than the absolute value of the density of the electrolyte solution. In this way, the influence of the water model on the simulation results was eliminated to a large extent,[22] and the ion models that were obtained can successfully be combined with different water models.[22] The resulting force fields for the alkali cations and halide anions describe well the experimental reduced density of all soluble alkali halide salts in aqueous solution over a wide composition and temperature range.[23] Using the SPC/E water model in combination with our ion force fields, the simulation results show a good agreement with the experimental self-diffusion coefficient of the ions, the hydration dynamics of water molecules around the ions and the enthalpy of hydration at 293.15 K and 298.15 K, respectively,[20] as well as with the electric conductivity over a wide temperature range.[23]

One of the most accurate methanol models[24] from the literature[25–28] is the model of Schnabel et al.[28] This model consists of two LJ sites and three partial charges and was obtained by readjusting the methanol model of van Leeuwen and Smit[27] to vapor-liquid equilibrium data of pure methanol,[28] namely the saturated liquid density, the vapor pressure and the enthalpy of vaporization. This model is known to accurately describe the density of pure methanol.[29] The temperature dependence of the density of pure liquid methanol at 1 bar is shown in Figure 1. The present simulation results are in very good agreement with experimental data (which were taken for test purposes from the present work and agree well with other published data[30]) over the entire investigated temperature range. The liquid density of methanol is only slightly overestimated by the force field with a deviation of around 0.1 %, cf. Figure 1. Although the same methanol force field was

used, the present simulation results of the density of pure methanol slightly differ from the data published by Guevara-Carrion et al.,[29] which can be attributed to the different applied long-range correction methods.

The thermodynamic properties of methanolic alkali halide salt solutions have been investigated in many simulation studies in the literature,[31–46] both by molecular simulation with classical force fields,[31–35,37–39,41,44–46] by Car-Parrinello molecular dynamics simulations[40,42,43] and by statistical perturbation theory.[36] In the molecular simulation studies, the thermodynamic properties of the methanolic electrolyte solutions were predicted, i.e. literature models were used, which were adjusted to properties of aqueous solutions in case of the ions (e.g. from Smith and Dang[10]) and to pure component properties in case of methanol (e.g. from Haughney et al.[26]), and no binary interaction parameters between the ions and the solvents were adjusted to the properties of the methanolic electrolyte solutions. Only Marx et al.[32] developed pair potentials for the ion-methanol and ion-ion interactions, which were derived from *ab initio* calculations.[32] In the literature studies both structural properties, e.g. the position of the first maximum in the radial distribution function of methanol around the ions,[31–34,36–46] and transport properties, e.g. the self-diffusion coefficient of the ions in methanolic electrolyte solutions[32,35,41,45,46] were investigated. However, to the best of our knowledge, the density of methanolic electrolyte solutions has not yet been studied by molecular simulation. Therefore, in the present work the density of methanolic alkali halide salt solutions is studied comprehensively by molecular simulation with the force fields for the ions[20,22] and methanol[28] developed in previous work of our group.

For such a comparison, plenty of experimental density data for various methanolic alkali halide salt solutions are available in the literature.[47–67] In Table 1, these publications are sorted according to the investigated alkali halide salts and temperatures. The survey shows that for many alkali halide salt solutions, there is a lack of experimental density data in the literature in the temperature (298.15 K - 313.15 K) and concentration (up to 0.05 mol/mol or 90 % of the solubility limit) range studied in the present work. At 298.15 K experimental density data are available from infinite dilution up to 90 % of the solubility limit for all alkali halide salt solutions except for sodium and

rubidium bromide as well as rubidium iodide solutions. For some alkali halide salt solutions small deviations can be observed between the data published by different authors. In other cases, data are only available from a single author (cf. Table 1). At the two other investigated temperatures, i.e. 308.15 K and 318.15 K, experimental density data are completely missing for several alkali halide salt solutions, cf. Table 1. In addition, the available literature data sets generally cover a very narrow concentration range. Solely the experimental density data of methanolic KI salt solutions published by Briscoe and Rinehart[49] (at 308.15 K and 318.15 K) and Gonzalez et al.[64] (at 308.15 K) cover the entire concentration range studied in this work. Hence, for the validation of the employed force field, the experimental density data from the literature had to be verified and extended.

For the present study, density measurements of the methanolic electrolyte solutions of all soluble alkali halide salts were conducted (LiF, NaF and RbF are insoluble in methanol). On this basis, gaps in the existing literature data are filled and a systematic comprehensive data set on densities of methanolic alkali halide salt solutions is provided. The density measurements were conducted at concentrations up to 0.05 mol/mol or 90 % of the solubility limit at temperatures of 298.15 K, 308.15 K and 318.15 K. Throughout this study all properties were investigated at 1 bar and the composition is given in terms of the ion mole fraction x_i, which is defined as

$$x_i = \frac{n_i}{2 \cdot n_i + n_{\mathrm{MeOH}}} \,, \tag{1}$$

where n_i is the mole number of each ion type and n_{MeOH} the mole number of methanol molecules in the electrolyte solution. For the 1:1 salt studied here, the ion mole fraction of the anions and the cations is x_i each. Some other studies quantify the salinity in terms of the salt mole fraction, regarding the salt as a single component. The ion mole fraction x_i is related to the overall salt mole fraction x_{S}

$$x_{\mathrm{S}} = \frac{n_{\mathrm{S}}}{n_{\mathrm{S}} + n_{\mathrm{MeOH}}} \tag{2}$$

by

$$x_S = \frac{x_i}{1 - x_i} \tag{3}$$

as the mole number of salt in the solution is $n_S = n_i$ here. Molecular simulations of methanolic electrolyte solutions were carried out at the same temperature, pressure and composition as in the experiments with the force fields of the ions[20,22] and methanol[28] developed in previous work of our group. The present simulation results are predictions as no interaction parameters were adjusted to the properties of the methanolic electrolyte solutions. The predictive capacity of the present employed ion force fields was validated regarding the reduced density, which is defined as

$$\widetilde{\rho} = \frac{\rho}{\rho_{\mathrm{MeOH}}} \,, \tag{4}$$

where ρ_{MeOH} is the density of pure methanol at the same temperature and pressure as the density of the solution ρ. It is used as reference property to minimize the influence of the uncertainty in the methanol model on the simulation results, although this error is rather small, cf. Figure 1. In case of experimental densities ρ, the density of pure methanol is taken from the present experimental data and in case of simulation results for the density of the solutions, ρ_{MeOH} is determined in pure methanol simulations. The simulation results and the experimental data of ρ are discussed individually for the different alkali halide salt solutions. Furthermore, structural, dynamic and transport properties of the methanolic electrolyte solutions were predicted by molecular simulation at 298.15 K and compared to experimental literature data where available.

In Section 2, the experiments are described. The employed force fields and the simulation methods are introduced in Section 3. In Section 4, the experimental data and the simulation results are presented and discussed. Section 5 summarizes the main statement from the present work.

2. Experimental Methods

The methanolic alkali halide salt solutions were prepared in a glove box in a water-free atmosphere. Dry air (provided by the ecodry KA-MT 2 system of Parker Hannifin) was continuously blown through the glove box. Additionally, the atmosphere in the box was dried with phosphorus pentoxide (P_2O_5). For the preparation of the electrolyte solution, ultradry (≤50 ppm water) methanol (Rotidry, Roth) with a purity of ≥99.9 % was used. The purity and the supplier of the alkali halide salts are shown in Table 2. The reagent grade alkali halide salts were dried at 353 K in a vacuum oven for 48 h before for each salt different samples of about 20 ml of desired concentrations x_i were prepared gravimetrically (AE240, Mettler-Toledo). The uncertainty of x_i, which was estimated by error propagation considering the resolution of the balance and the error by determining the concentrations gravimetrically, was found to be for all samples below ±0.00001 mol/mol. Information of the solubility limit of alkali halide salts in methanol is available in the literature.[68–79] Here, the data of Pavlopoulos and Strehlow[71] (for LiCl, LiBr, LiI, rubidium and cesium halide salts) and Harner et al.[72] (for LiF, sodium and potassium halide salts) were used as their work covers in each case a wide range of alkali halide salts and their data proved to be reliable during the present experiments.

The density of the electrolyte solutions was determined with a vibrating tube densimeter (DMA 4500M, Anton Paar). Based on the resolution of the densimeter and results from the repetition of experiments at the same conditions, the uncertainty of the density measurements was found to be better than ±0.0001 g/cm^3. The uncertainty of the temperature measurements is reported to be better than ±0.1 K. The densimeter was initially calibrated with air and deionized liquid water (produced by the Elix Essential 5^{UV} of Merck Millipore), which was degased before use by boiling.

3. Molecular simulation

In this study, rigid, non-polarizable force fields of the LJ (ions) and united-atom LJ (MeOH) type with superimposed point charges were used. The force fields for methanol[28] and the alkali cations and halide anions[20,22] were taken from previous work of our group. The methanol model is composed of two united-atom LJ sites accounting for repulsion and dispersion of the methyl and the hydroxyl group as well as three point charges. These are located in the center of the methyl group and at the position of the oxygen and hydrogen atom of the hydroxyl group to model both polarity and hydrogen bonding. The geometry of the methanol force field is illustrated in Figure 2 and the parameters are listed in Table 3. The ion force fields consist of one LJ site with a superimposed point charge of ±1 e in the center of mass. Their LJ parameters are listed in Table 4.

The potential energy u_{ij} between two molecules i and j consisting of $N_{\mathrm{S},i}$ and $N_{\mathrm{S},j}$ interaction sites is given by

$$u_{ij} = \sum_{a=1}^{N_{\mathrm{S},i}} \sum_{b=1}^{N_{\mathrm{S},j}} \left[4\varepsilon_{ab} \left(\left(\frac{\sigma_{ab}}{r_{ab}} \right)^{12} - \left(\frac{\sigma_{ab}}{r_{ab}} \right)^{6} \right) + \sum_{l=1}^{N_{\mathrm{C},a}} \sum_{m=1}^{N_{\mathrm{C},b}} \frac{q_l q_m}{4\pi\varepsilon_0 r_{lm}} \right] , \tag{5}$$

where a and b is the site index of molecule i and j, respectively. r_{ab} represents the distance between the interaction sites a and b. σ_{ab} and ε_{ab} are the LJ size and energy parameters. q_l and q_m are the charges of the solute or the solvent particles that are at a distance r_{lm} and ε_0 is the vacuum permittivity. The indices l and m enumerate the point charges, while the total number of charges of site a is $N_{\mathrm{C},a}$. Note that Eq. (5) is given in a form that includes all interactions, i.e. solvent-solvent, ion-solvent and ion-ion. In mixtures of polar and charged molecules, the electrostatic contribution to the unlike interaction is fully determined by the laws of electrostatics. For the unlike LJ parameters, the Lorentz-Berthelot[80,81] combining rules were employed

$$\sigma_{ab} = \frac{\sigma_{aa} + \sigma_{bb}}{2} , \tag{6}$$

$$\varepsilon_{ab} = \sqrt{\varepsilon_{aa}\varepsilon_{bb}} . \tag{7}$$

No interaction parameters between the ions and the solvent were adjusted to properties of methanolic electrolyte solutions. Hence, the simulation results presented in this study are throughout predictions.

In the present study, the radial distribution function $g_{i-\mathrm{O}}(r)$ of the hydroxyl and $g_{i-\mathrm{CH3}}(r)$ of the methyl group around the ion i, the solvation number $n_{i-\mathrm{O}}$ and the residence time $\tau_{i-\mathrm{O}}$ of methanol molecules in the first solvation shell around the ion, the self-diffusion coefficient D_i of the ions and the electric conductivity σ of the solution were determined by molecular simulation at 298.15 K. The methods for the calculation of the RDF,[82] $n_{i-\mathrm{O}}$[83] and $\tau_{i-\mathrm{O}}$[84] are well-known and established. For the determination of $g_{i-\mathrm{O}}(r)$ the position of the hydroxyl group and for $n_{i-\mathrm{O}}$ and $\tau_{i-\mathrm{O}}$ the position of the methanol molecule is represented by the position of the oxygen atom, which is widely applied in simulation studies in the literature, e.g. by Chowdhuri and Chandra.[41]

Following a proposal by Impey et al.,[85] unpairing of an ion and a methanol molecule was defined to occur if their separation lasted longer than the residence time $\tau_{\mathrm{O}-\mathrm{O}}$ of a methanol molecule around a neighboring molecule in a pure bulk methanol simulation at the same conditions. However, for short-time pairing of two particles no such restrictions exist.[85] The period of short-time pairing is used without further modifications for the calculation of the ensemble average of $\tau_{i-\mathrm{O}}$.

The self-diffusion coefficient of the ions and the electric conductivity of the methanol solutions were determined via equilibrium molecular dynamics (MD) simulations by means of the Green-Kubo formalism.[86,87] This formalism establishes a direct relationship between a transport coefficient and the time integral of the autocorrelation function of the corresponding flux within a fluid. The Green-Kubo expression for the self-diffusion coefficient D_i is based on the individual ion velocity autocorrelation function[88] and the electric conductivity σ is related to the time autocorrelation function of the electric current flux $\boldsymbol{j}(t)$.[89]

For all simulations carried out in this work, the simulation program *ms2*[90] was used. Technical details are given in the Appendix: Simulation details.

4. Results and discussion

4.1 Experimental data

The experimental density data are listed in Footnote for methanolic alkali halide salt solutions as well as for pure liquid methanol.

In Figure 3 and Figure 4 the present experimental density data of the methanolic electrolyte solutions are compared to literature data at 298.15 K (cf. Table 1) over the entire investigated composition range. Only data sets which cover exclusively very dilute solutions, e.g. the data published by Takenaka et al.,[59–61] are not shown and considered in the following discussion.

The present experimental data are in excellent agreement with the literature data over the entire investigated composition range, cf. Figure 3 and Figure 4. The deviations are generally below 0.1 %. For NaBr, NaI, KCl, KBr, RbBr, RbI, CsF, CsCl and CsBr salt solutions the observed deviations are even below 0.05 %. An exceptional case is LiI where deviations up to 0.17% from the data of Renz[56] were found at the highest investigated concentration. In case of LiBr, the deviations from the data of Pasztor et al.[53] are 0.3% at the highest concentration whereas the deviation from the remaining literature data[51,58,63] is below 0.1 %. The deviations from the data of Gonzalez et al.[64] in case of KI increase up to 1.16 % at the highest concentration. According to Figure 3, these data possess an increasing mismatch both to the present experimental data and the remaining literature data.[47–50,52,53,58,61,62] The deviation between these other data and the present experimental data is below 0.1 %. Furthermore a deviation up to 0.13% from the data of Werblan[54] were found in case of CsCl. However, the present experimental data for methanolic CsCl salt solutions are in excellent agreement with the data of Kawaizumi and Zana[52] (deviations below 0.05 %).

For the two other studied temperatures (308.15 K and 318.15 K) only scarce data are available (cf. Table 1) and hence the comparison between the present experimental and literature data is not shown graphically. The deviation between present experimental and literature data is for all alkali halide salt solutions at both temperatures below 0.05 %. An exceptional case is KI at 308.15 K

where the deviation from the data of Gonzalez et al.[64] increases up to 1.63 % at the highest concentration, whereas the deviation from the data of Figurski and Nipprasch[62] and Briscoe and Rinehart[49] is below 0.1 % and 0.05 %, respectively.

The density of the electrolyte solutions ρ increases linearly with the ion mole fraction x_i for a given temperature in the concentration range studied in this work, cf. Figure 3 and Figure 4 and Footnote . The corresponding data of the slope a of ρ over x_i with

$$\rho = \rho_{\mathrm{MeOH}} + a \cdot x_i \tag{8}$$

at 298.15 K and 318.15 K are listed in Table 6. For all lithium and sodium halide salts, the standard deviation $\Delta\rho$ of the correlation for the density of the methanolic electrolyte solutions, cf. Eq. (8), is smaller than ±0.001 g/cm^3. For the potassium, rubidium and cesium halides $\Delta\rho$ is even smaller than ±0.0002 g/cm^3. The slope a is individual for the different alkali halide salts and is almost independent on the temperature (cf. Table 6). Hence, the temperature dependence of the density of the methanolic electrolyte solutions studied here is only determined by the temperature dependence of pure methanol, cf. Footnote . Hence, the reduced density $\widetilde{\rho}$ of the electrolyte solution is also almost independent on the temperature.

4.2 Comparison of simulation results to experimental data

The simulation results of the density ρ of the methanolic alkali halide salt solutions as well as of pure liquid methanol are listed in Table 7.

In Figure 5 and Figure 6, the simulation results of the reduced density $\widetilde{\rho}$ at 298.15 K and 318.15 K are compared to the present experimental data. At 298.15 K, the simulation results are in excellent agreement with the experimental data over the entire investigated concentration range. The deviations are throughout below 0.4 %, except for LiCl and LiBr salt solutions where the deviations are up to 1 % at the highest investigated concentration, cf. Figure 5. The simulation results for $\widetilde{\rho}$ are

found to be almost temperature-independent, which is consistent with the experimental data, cf. Figure 5 and Figure 6.

The simulation results of the density of the electrolyte solutions ρ increase, at a given temperature, linearly with the ion mole fraction x_i. The slope a of the different alkali halide salt solutions determined from the simulation results of ρ are compared to experimental data at 298.15 K and 318.15 K in Figure 7. Analogous to the experimental data, the predictions of a from molecular simulation are found to be almost independent on the temperature. The discontinuous decrease of a with increasing atomic number of the ions (e.g. identical slopes a for sodium and potassium halide salt solutions) can be attributed to a superposition of the increasing ion size and mass and the influence of the ion on the hydrogen bonding network of the surrounding methanol molecules. The discussion of the effect of the ions on the solvent hydrogen bonds is beyond the scope of this study.

4.3 Structural properties

The RDF of the oxygen atom $g_{i-\mathrm{O}}(r)$ and the methyl group $g_{i-\mathrm{CH3}}(r)$ of methanol around the alkali cations and halide anions in methanolic solution was determined by molecular simulation at 298.15 K and low salinity (x_i = 0.002 mol/mol). Hence, the results of $g_{i-\mathrm{O}}(r)$ and $g_{i-\mathrm{CH3}}(r)$ around the single ions are almost independent on the counterion in the solution. The RDF of the oxygen atom and the methyl group of methanol around the ions was determined for LiCl, NaBr, KF, RbI and CsCl salt solutions.

The simulation results of the RDF $g_{i-\mathrm{O}}(r)$ and $g_{i-\mathrm{CH3}}(r)$ are listed in Table 8 and are shown exemplarily for the cesium cation and the fluoride anion in Figure 8. Both for the cation and the anion, the position of the first maximum $r_{\mathrm{max},1}$ of $g_{i-\mathrm{O}}(r)$ is closer to the ion than of $g_{i-\mathrm{CH3}}(r)$. Hence, in both cases the hydroxyl group of the methanol molecule points towards the ion and the methyl group generally faces into the opposite direction. This orientation was also observed in simulation studies in the literature.[31–33,44] The comparison between the position of the first maximum $r_{\mathrm{max},1}$

in the RDF $g_{i-\mathrm{O}}(r)$ of the oxygen atom of the methanol molecule and of the SPC/E water model (published by Reiser et al.[20]) around the ions reveals that $r_{\mathrm{max},1}$ for the different ions is identical in aqueous and methanolic electrolyte solutions. This was also observed both in simulation studies[44,46] and from the comparison of experimental $g_{i-\mathrm{O}}(r)$ data.[91] The good agreement between the experimental data and the predictions from molecular simulation of the reduced density of the alkali halide salt solutions (cf. Section 4.2) can be directly attributed to the identical values of $r_{\mathrm{max},1}$ for $g_{i-\mathrm{O}}(r)$ in aqueous and methanolic solutions. The density is strongly influenced by the microscopic structure, which is identical in the surrounding of the ion in aqueous and methanolic salt solutions. Hence, the ion models adjusted in aqueous solution possess the capability to predict well the density of methanolic alkali halide salt solutions.

The position of the first maximum $r_{\mathrm{max},1}$ in the RDF $g_{i-\mathrm{O}}(r)$ and $g_{i-\mathrm{CH3}}(r)$ is shown in Figure 9. The simulation results are in good agreement with the experimental data from the literature[92,93] where available. The deviations are both for $g_{i-\mathrm{O}}(r)$ and $g_{i-\mathrm{CH3}}(r)$ generally below 13 %, except for $g_{\mathrm{Li-CH3}}$ where deviations up to 20% were observed. The size parameters of the Li^+ and Na^+ models are almost identical (σ_{Li}=1.88 Å, σ_{Na}=1.89 Å) and hence the same position of the first maximum $r_{\mathrm{max},1}$ in the RDF of the oxygen atom and the methyl group around both ions, respectively, was found. The position $r_{\mathrm{max},1}$ increases both for $g_{i-\mathrm{O}}(r)$ and $g_{i-\mathrm{CH3}}(r)$ in linear fashion with increasing size of the ions. The slope of the increase is in both cases identical for the cations and the anions and, furthermore, almost identical for $g_{i-\mathrm{O}}(r)$ and $g_{i-\mathrm{CH3}}(r)$. Comparing the position of the first maximum around the cesium anion and the only slightly larger fluoride anion, a decrease of $r_{\mathrm{max},1}$ is observed both in the RDF $g_{i-\mathrm{O}}(r)$ and $g_{i-\mathrm{CH3}}(r)$, cf. Figure 9. This decrease can be attributed to the different orientations of the methanol molecules around the ions.

$g_{i-\mathrm{O}}(r)$: In case of the positively charged cesium ion, the negatively charged oxygen atom of the methanol molecules points towards the cation and the positively charged hydrogen atom of the hydroxyl group and the methyl group face into the opposite direction.[32,33,44] Because these equally charged parts of neighboring methanol molecules lead to a mutual repulsion, the methanol molecules are not able to form a strongly attached solvation shell around the cesium cation. In

comparison, only the hydrogen atom of the hydroxyl group points towards the negatively charged fluoride ion.[32,33,44] The methyl group, which is turning away from the ion, is attracted by the oxygen atom of a neighboring methanol molecule. Hence, the methanol molecules constitute a more firmly attached solvation shell around the fluoride anion which is closer to the ion.

$g_{i-\mathrm{CH3}}(r)$: Besides the above described effect of the charges on the methanol molecules in the solvation shell, the position of $r_{\mathrm{max},1}$ of $g_{i-\mathrm{CH3}}(r)$ is also influenced by a further aspect. In case of the cesium cation, the positively charged methyl group of the methanol molecules is forced by electrostatic repulsion to face away from the equally charged ion in the solvation shell. In contrast, the methyl group is attracted by the charge of the fluoride anion and is, hence, significantly closer to the ion in the solvation shell, cf. Figure 9.

4.4 Solvation number

The solvation number $n_{i-\mathrm{O}}$ of methanol molecules in the first solvation shell around the ions was evaluated at 298.15 K. The basis of the calculation of the solvation number is the RDF $g_{i-\mathrm{O}}(r)$ from the previous section. Hence, the results of $n_{i-\mathrm{O}}$ are almost independent on the counterion in the solution.

The simulation results of $n_{i-\mathrm{O}}$ around the different alkali cations and halide anions in methanolic solutions are shown in Figure 10 and are listed in Table 9. For the alkali cations, an increase of the simulation results of $n_{i-\mathrm{O}}$ is observed, whereas for the halide anions a decrease with increasing size of the ions is observed. The same contrast was also observed by Chowdhuri and Chandra[41] in their systematic simulation study of the solvation number around all alkali cations and halide anions. For all ions, the present simulation results of $n_{i-\mathrm{O}}$ are in good agreement with the data published by Chowdhuri and Chandra[41] and with other simulation data from the literature, i.e. of $n_{i-\mathrm{O}}$ around Na^+,[32,33,36,38,43,44] K^+,[36,43] and Cl^-.[31–33,38,40,44]

The comparison between the simulation results and experimental data from the literature,[92,93] where available, reveals, that $n_{i-\mathrm{O}}$ is well predicted around all ions by molecular simulation, cf. Figure 10. The deviations are below 11 % except for the solvation number around the iodide anion

where a deviation from the experimental data of 35 % is observed. However, the decrease of n_{i-O} with increasing size of the anions, which was observed in simulation studies, can not be observed in the experimental studies, cf. Figure 10.

4.5 Solvation dynamics

The residence time τ_{i-O} of the methanol molecules around the ions was determined by MD simulation at 298.15 K. The residence time was sampled in the same methanolic electrolyte solutions and under the same conditions as the RDF, cf. Section 4.3. Hence, the results of τ_{i-O} are almost independent on the counterion in the electrolyte solution.

For the simulation of τ_{i-O}, the residence time of a methanol molecule around a neighboring molecule in pure bulk methanol τ_{O-O} was required (cf. Section 3). It was determined by MD simulation at the same conditions and was found to be τ_{O-O} = 1.7 ps. This period of short time unpairing of ion and methanol molecule, which is fully accounted to the calculation of τ_{i-O}, is consistent with the findings of Hawlicka and Rybicki.[44]

The simulation results of the residence time τ_{i-O} of methanol around the different ions are listed in numerical form in Table 9. The residence times τ_{i-O} decrease with increasing size both of the cations and the anions, cf. Table 9. With increasing size of the ion the electrostatic interaction between the ions and the methanol molecules decreases and hence the methanol molecules are more likely to leave the solvation shell. Because of the different orientations of the methanol molecules around the cations and the anions (cf. Section 4.3), the methanol molecules form a more strongly bonded solvation shell around the fluoride anion than around the cesium cation, although these ions have almost the same size. Hence, the residence time τ_{F-O} is significantly larger then τ_{Cs-O}, cf. Table 9. In the literature, a systematic study of the residence times τ_{i-O} of methanol around all alkali cations and halide anions is missing. In simulation studies, τ_{i-O} was determined in methanolic NaCl[33,35] and LiCl[46] salt solutions. The present simulation results of τ_{Na-O} are in between the data reported by Hawlicka and Swiatla-Wojcik[35] and Sese at al.[33] However, the present simulation

results of $\tau_{\mathrm{Cl-O}}$ are below the data published by Kumar et al.,[46] Hawlicka and Swiatla-Wojcik[35] and Sese at al.[33] The same was also observed for $\tau_{\mathrm{Li-O}}$ in comparison to the data reported by Kumar et al.[46]

4.6 Self-diffusion coefficient

The self-diffusion coefficient D_i of all alkali cations and halide anions in methanolic solution was determined at 298.15 K and low salinity (x_i = 0.001 mol/mol). Hence, the influence of correlated motion between anion and cation in the solution is low and D_i is almost independent on the counterion type in the solution.

The self-diffusion coefficients of the alkali cations and halide anions in methanolic solution are shown in Figure 11 and are listed in Table 9. The overall agreement between experimental data[94] and the predictions from molecular simulation is good. The highest deviation of 15 % is found in case of D_I. In the present simulations, the self-diffusion coefficients D_i increase with increasing size both of the cations and the anions. The same qualitative trend was also observed by Chowdhuri and Chandra[41] in their systematic study of D_i of all alkali cations and halide anions. However, a mismatch is found for the bigger halide anions, i.e. Br^- and I^-. In the experimental data[94] and the simulation study of Chowdhuri and Chandra,[41] the self-diffusion coefficient of the halide anions increases continuously from D_{F} up to D_{I}. In case of the present simulation this trend is only observed from F^- to Cl^-. The self-diffusion coefficients D_{Br} and D_{I} are found to be almost identical to D_{Cl}.

The dependence of D_i on the size of the ion is directly linked to the formation of ion-methanol complexes that typically dominates the ion motion within the solution.[20] With increasing size of the ion, the influence of the charge on surrounding methanol molecules decreases and the formation of the ion-methanol complex is less pronounced. Hence, the effective radius of the ion-methanol complex decreases and the ion mobility increases. The comparison between the self-diffusion coefficients of Cs^+ and F^-, which have almost the same size, reveals that D_i and hence the ion

mobility is higher in case of the alkali cation. This can be attributed to the different orientation of the methanol molecules in the solvation shell around the oppositely charged ions. For F^-, the methanol molecules in the solvation shell are strongly attached to the ion which leads to a bigger effective radius of the ion-methanol complex and hence a smaller self-diffusion coefficient (see Section 4.3 for a discussion of the orientation of the methanol molecules around the cations and the anions).

4.7 Electric conductivity

The electric conductivity σ of methanolic lithium, sodium and potassium chloride, bromide and iodide salt solutions were calculated at various ion mole fractions at 298.15 K (except LiBr at 293.15 K). These specific salts were chosen because sufficient experimental data were available in the literature.[95–100] The concentration range of the literature data prescribes the investigated concentrations of the alkali halide salt solutions. The availability of experimental literature data[95] is also the reason for the slightly different temperature in case of the LiBr salt solutions.

The electric conductivity of the different methanolic alkali halide salt solutions is shown in Figure 12. The predictions from molecular simulations are in good agreement with the experimental data.[95–100] The deviations are generally below 15 %, for KCl and LiI salt solutions even below 10 %. An exceptional case are the simulation results for the KI salt solutions, where deviations from the experimental data of about 27 % are found over the entire investigated concentration range .

5. Conclusions

The density of all methanolic alkali halide salt solutions was determined both by experiment and molecular simulation from 298.15 K to 318.15 K at 1 bar in a concentration range up to 0.05 mol/-

mol or 90 % of the solubility limit. Furthermore, the radial distribution function of the methanol sites around the ions, the solvation number and residence time of methanol molecules in the first solvation shell around the ions, the self-diffusion coefficient of the ions and the electric conductivity was investigated by molecular simulation. The molecular models for the simulations were taken from previous work of our group and were therein adjusted in case of the alkali cations and halide anions to properties of aqueous solutions and in case of the solvent methanol to pure component properties. The simulation results in this work are throughout predictions as no interaction parameters between the ions and the solvent were adjusted to properties of methanolic electrolyte solutions.

The density measurement results of the methanolic alkali halide salt solutions are in excellent agreement with data from the literature. Prior to this work, there was a lack of experimental data in the concentration range considered in this study for sodium and rubidium bromide as well as rubidium iodide solutions at 298.15 K and for all alkali halide salt solutions at 308.15 K and 318.15 K except for KI salt solutions. The predictions from molecular simulation of the slope a and the reduced density $\widetilde{\rho}$ are in good agreement with the experimental data for all alkali halide salt solutions. The experimental data of a and $\widetilde{\rho}$ are found to be almost independent on the temperature, which is predicted correctly by the molecular simulation.

The simulation results of the position of the first maximum $r_{\mathrm{max},1}$ in the RDF of the hydroxyl group $g_{i-\mathrm{O}}(r)$ and the methyl group $g_{i-\mathrm{CH3}}(r)$ of the methanol molecule as well as of the number of methanol molecules in the first solvation shell around the ion $n_{i-\mathrm{O}}$ are found to be generally in good agreement with experimental data from the literature, as far as such data are available. The differences in the positions $r_{\mathrm{max},1}$ around Cs^+ and F^-, which have almost the same size, can be attributed to the different orientations of the methanol molecules around the cations and the anions. The residence time of methanol molecules in the first solvation shell around the ions $\tau_{i-\mathrm{O}}$ decreases with increasing size of the ions as the electrostatic attraction between ion and solvent decreases. Hence, the molecules in the hydration shell are weaker bonded. The different orientations of the methanol molecules lead in case of the fluoride anion to a stronger bonded solvation shell with a

smaller value of $\tau_{i-\mathrm{O}}$ in comparison to the cesium cation.

The predictions from molecular simulation of the self-diffusion coefficients D_i of the alkali cations and halide anions and of the electric conductivity σ of numerous alkali halide salt solutions are in good agreement with experimental literature data, where available. The increase of D_i with increasing size of the ions can be attributed to the decreasing effective radius of the ion-methanol complex, which typically dominates the mobility of the ion in the solution.

The present study of methanolic electrolyte solutions generalizes our previous work on aqueous electrolyte solutions.[23] On this basis, the thermodynamic properties and their simulation results can easily be compared for aqueous and methanolic alkali halide salt solutions.

Acknowledgments

The authors gratefully acknowledge financial support within the Reinhart Koselleck Program (HA1993/15-1) of the German Research Foundation (DFG). The present work was supported computationally by the Regional University Computing Center (RHRK) under the grant MSWS and the High Performance Computing Center Stuttgart (HLRS) under the grant MMHBF2. It was conducted under the auspices of the Boltzmann-Zuse Society of Computational Molecular Engineering (BZS).

Appendix: Simulation details

All simulations of this study were carried out with the simulation program *ms*2.[90] In *ms*2, thermophysical properties can be determined for rigid molecular models using Monte-Carlo (MC) or molecular dynamics (MD) simulation techniques. For all simulations, the LJ interaction partners are determined for every time step and MC loop, respectively. Interaction energies between molecules and/or ions are determined explicitly for distances smaller than the cut-off radius r_{c}. The thermostat incorporated in *ms*2 is velocity scaling. The pressure is kept constant using Andersen‘s barostat in MD, and random volume changes evaluated according to Metropolis acceptance

criterion in MC, respectively. The simulation uncertainties were estimated with the block average method by Flyvberg and Petersen.[101]

The liquid density of methanolic alkali halide solutions was determined with the MC technique in the isothermal-isobaric (NpT) ensemble at a constant pressure of 1 bar for different temperatures and compositions. Depending on the composition, the simulation volume contained 2 to 50 cations. The molecule number in the simulations was set at least to $N = 1000$ and increased up to $N = 1364$. A physically reasonable configuration was obtained after 5000 equilibration loops in the canone ensemble (NVT), followed by $80,000$ relaxation loops in the NpT ensemble. Thermodynamic averages were obtained by sampling $512,000$ loops. Each loop consisted of $N_{\mathrm{NDF}}/3$ steps, where N_{NDF} indicates the total number of mechanical degrees of freedom of the system. Electrostatic long range contributions were considered by Ewald summation[102] with a real space convergence parameter $\kappa = 5.6$. The real space cut-off radius was equal to the LJ cut-off radius of 19 Å.

For the calculation of structural and dynamic properties of the methanolic electrolyte solutions, MD simulations were carried out. In a first step, the density of the methanolic alkali halide solution was determined by an NpT simulation at the desired temperature, pressure and composition. Subsequently, the self-diffusion coefficient, the radial distribution function and the residence time were calculated in the NVT ensemble at the same temperature and composition with the density resulting from the first step. In these MD simulations, Newton‘s equations of motion were solved with a Gear predictor-corrector scheme of fifth order with a time step of 1.2 fs. The long-range interactions were considered by Ewald summation.[102]

The self-diffusion coefficient of the ions[88] and the electric conductivity of the solution[89] were calculated with the Green-Kubo formalism.[86,87] For simulations in the NpT ensemble, a physically reasonable configuration was attained by $10,000$ time steps in the NVT ensemble and $100,000$ time steps in the NpT ensemble, followed by a production run over $800,000$ time steps. In the NVT ensemble, the equilibration was carried out over $150,000$ time steps, followed by a production run of $6,000,000$ time steps for the calculation of the self-diffusion coefficient and the electric conduc-

tivity. The sampling length of the velocity and the electric current autocorrelation functions was set to 14 ps and the separation between the origins of two autocorrelation functions was 0.15 ps. Within this time span, all correlation functions decayed to less than 1/e of their normalized value. The MD unit cell with periodic boundary conditions contained 5000 molecules. This relative high number of molecules was used here to minimize the influence of the finite size effect on the simulation results. Using the Green-Kubo formalism[86,87] for the calculation of transport properties of aqueous systems, Guevara-Carrion et al.[103] showed that the finite site effect saturates with increasing number of molecules. No significant differences were observed above 2048 molecules.[103] For the calculation of the self-diffusion coefficient, the simulation volume contained 4990 methanol molecules, 5 alkali ions and 5 halide ions. The electric conductivity was determined for different compositions. Hence, the number of ions in the simulation volume varied from 4 to 115. The real space and LJ cut-off radius was set to 30 Å.

The radial distribution function and the residence time were determined by molecular simulation of systems containing 2 cations, 2 anions and 996 methanol molecules. For simulations in the NpT ensemble, the system was equilibrated over $10,000$ time steps in the NVT ensemble and $100,000$ time steps in the NpT ensemble, followed by a production run over $2,000,000$ time steps. The resulting density was used in a subsequent NVT ensemble simulation for the determination of the RDF of methanol around the ions. The RDF was sampled up to a cut-off radius of 19 Å with 645 bins. The results for the position of the first minimum of the RDF were used in a second NVT ensemble simulation with the same density for the determination of the residence time of methanol molecules around the ions. In both NVT simulations, the system was equilibrated over $100,000$ time steps, followed by a production run of $1,000,000$ time steps.

The same process was applied for the calculation of the pure methanol properties, i.e. the self-diffusion coefficient and the residence time of methanol molecules around themselves.

Figure 1: Density of pure liquid methanol as a function of the temperature at 1 bar. Simulation results from the present work (◆) are compared to present experimental data (○). The line indicates a correlation of experimental data from the literature.[30]

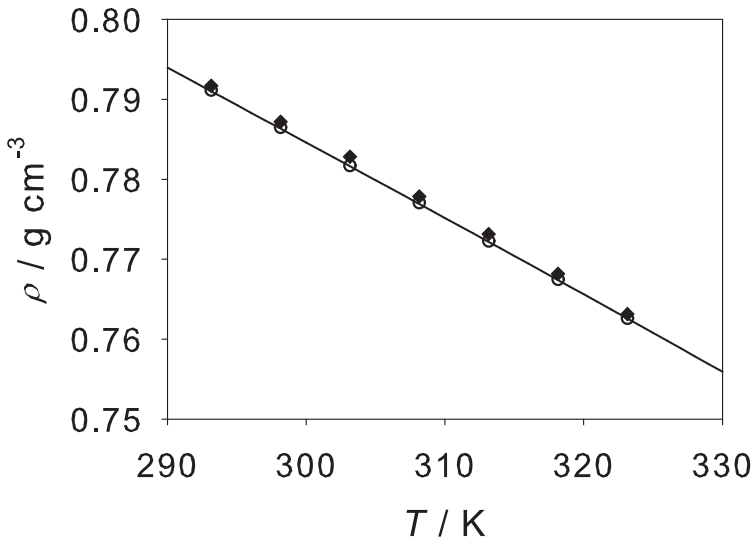

Figure 2: Geometry of the methanol model by Schnabel et al.:[28] S_i indicates the model interaction site i.

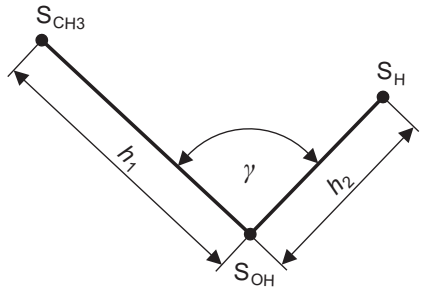

Figure 3: Density of methanolic lithium and sodium halide, potassium fluoride and iodide and rubidium iodide salt solutions as a function of the ion mole fraction at 298.15 K and 1 bar. Present experimental data (●) are compared to data from the literature: Skabichevskii[51](△), Vosburgh et al.[47](☆), Kiepe et al.[63](○), Pasztor and Criss[53](△), Lankford et al.[58](▽), Renz[56](▽), Jones and Fornwalt[48](☆), Wawer et al.[67](+), Figurski and Nipprasch[62](◇), Gonzalez et al.[64](○), Briscoe and Rinehart[49](◇), Eliseeva et al.[65](×), Werblan[54] (□) and Kawaizumi and Zana[52](□).

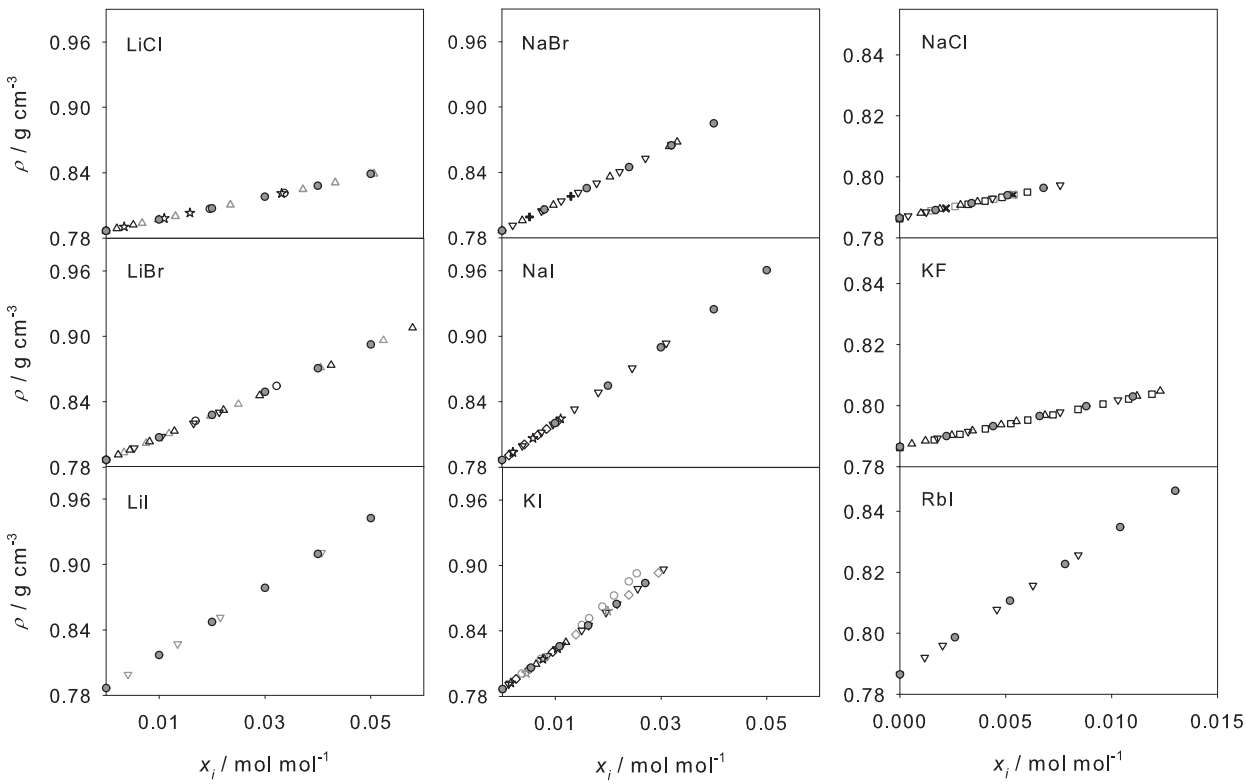

Figure 4: Density of methanolic potassium and rubidium chloride and bromide and cesium halide salt solutions as a function of the ion mole fraction at 298.15 K and 1 bar. Present experimental data (•) are compared to data from the literature: Lankford et al.[58](▽), Kawaizumi and Zana[52](□), Vosburgh et al.[47](☆), Kolhapurkar et al.[66] (×), Pasztor and Criss[53](△), Werblan[54,55] (□) and Figurski and Nipprasch[62](◇).

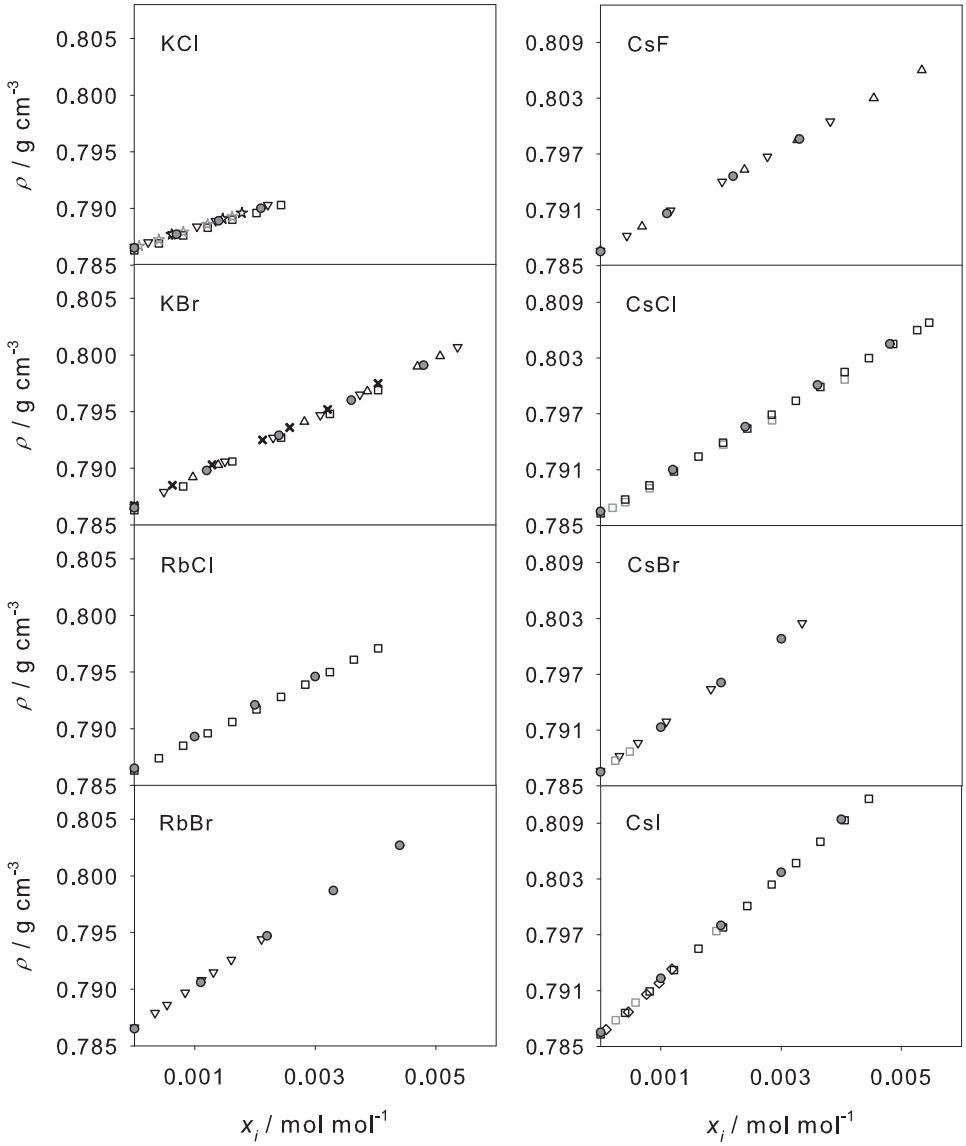

Figure 5: Reduced density of methanolic lithium and sodium halide, potassium fluoride and iodide and rubidium iodide salt solutions as a function of the ion mole fraction at 1 bar. Present simulation data (symbols) are compared to correlations of the present experimental data (lines): 298.15 K (○, —) and 318.15 K (×, ···). For several solutions the lines and symbols of the different temperatures lie upon each other.

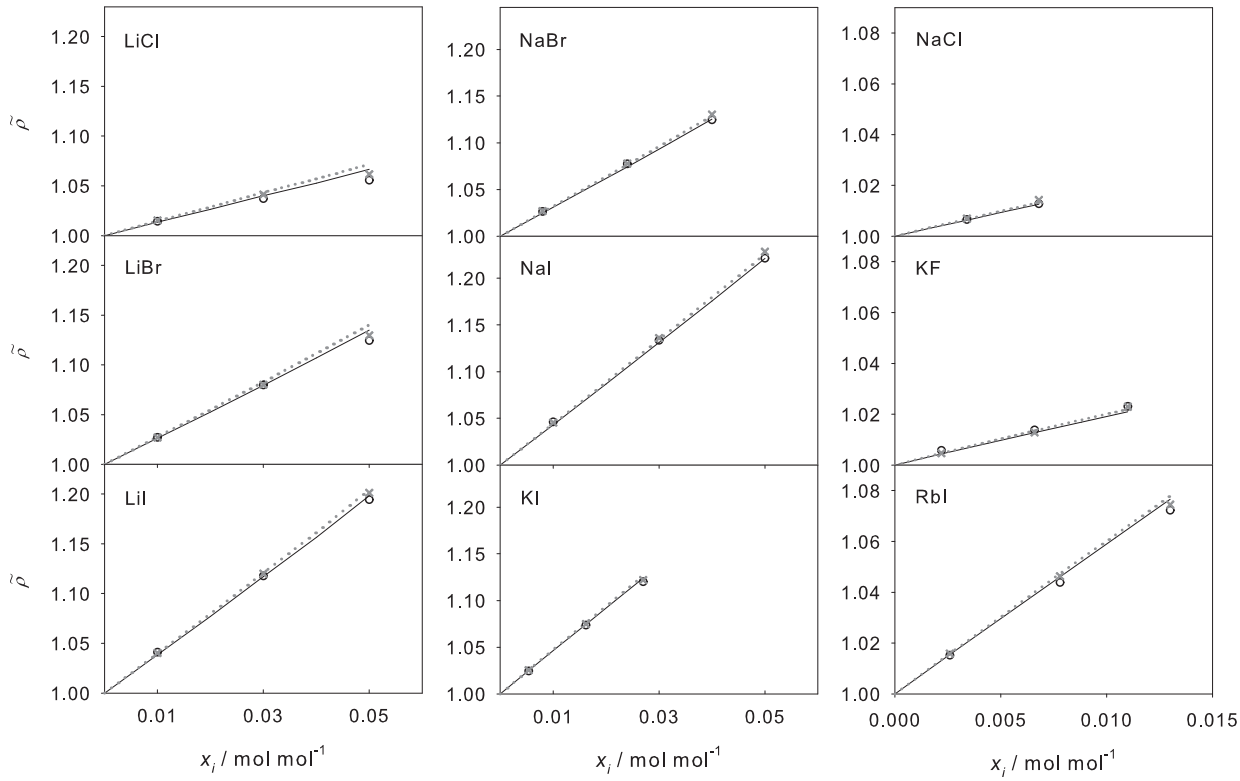

Figure 6: Reduced density of methanolic potassium and rubidium chloride and bromide and cesium halide salt solutions as a function of the ion mole fraction at 1 bar. Present simulation data (symbols) are compared to correlations of the present experimental data (lines): 298.15 K (∘, —) and 318.15 K (×, ···). For several solutions the lines and symbols of the different temperatures lie upon each other.

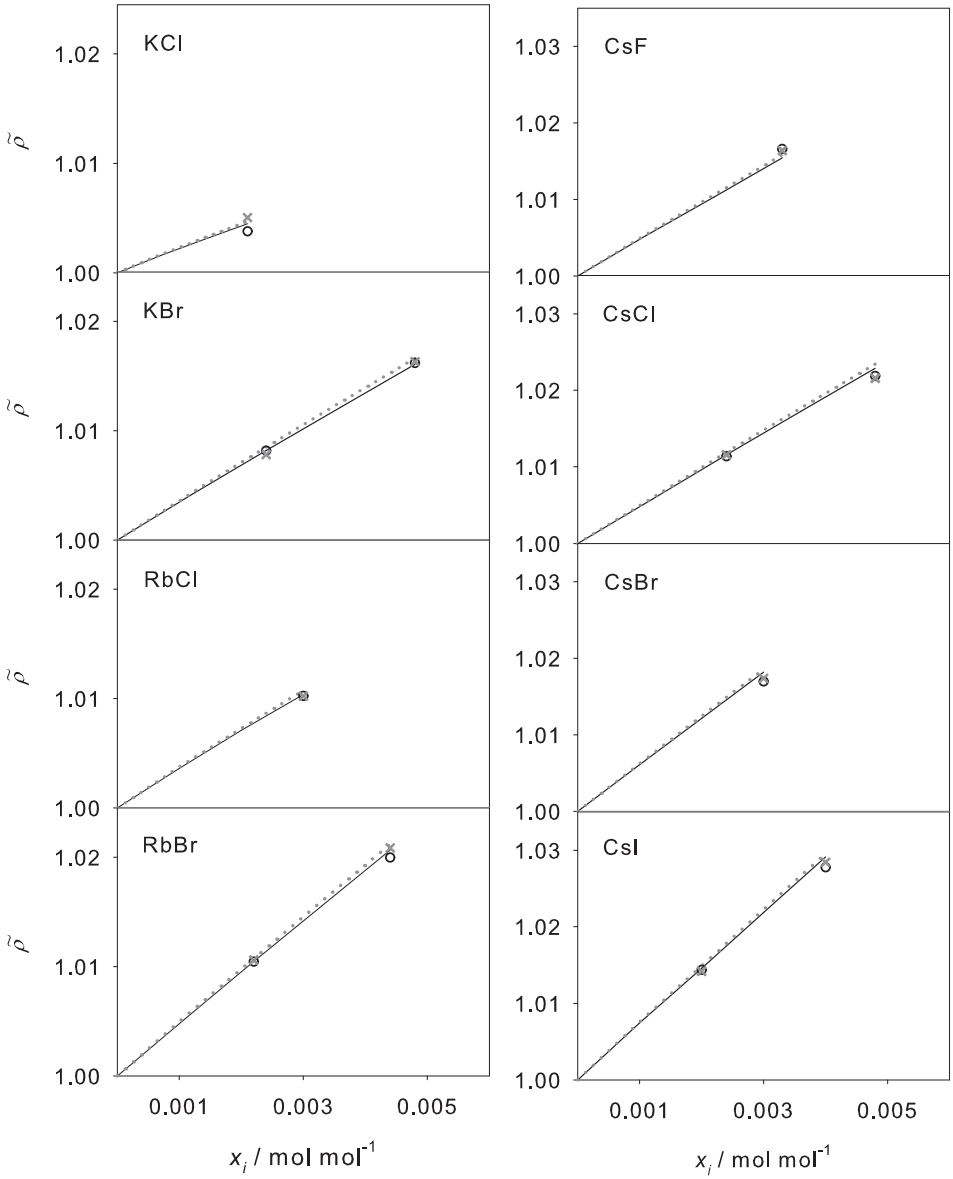

Figure 7: Slope of the density of methanolic alkali halide salt solutions over the ion mole fraction at 1 bar. Present simulation data (symbols) are compared to present experimental data (lines): 298.15 K (∘, —) and 318.15 K (×, ···). For several solutions the lines and symbols of the different temperatures lie upon each other.

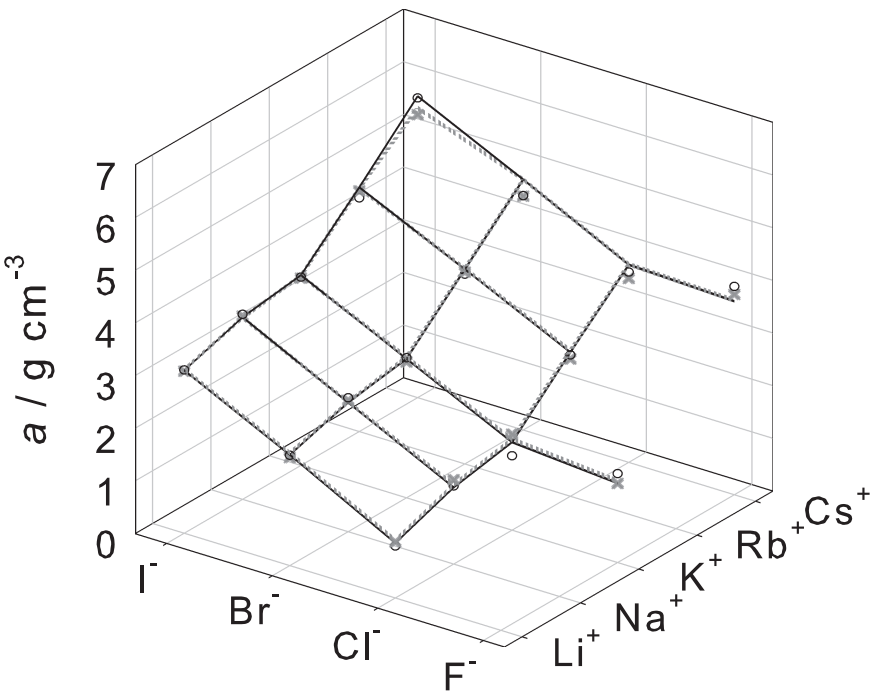

Figure 8: Radial distribution function of the oxygen atom (—) and the methyl group (- - -) of methanol around Cs^+ (top) and F^- (bottom) in methanolic solution (x_i=0.002 mol/mol) at 298.15 K and 1 bar.

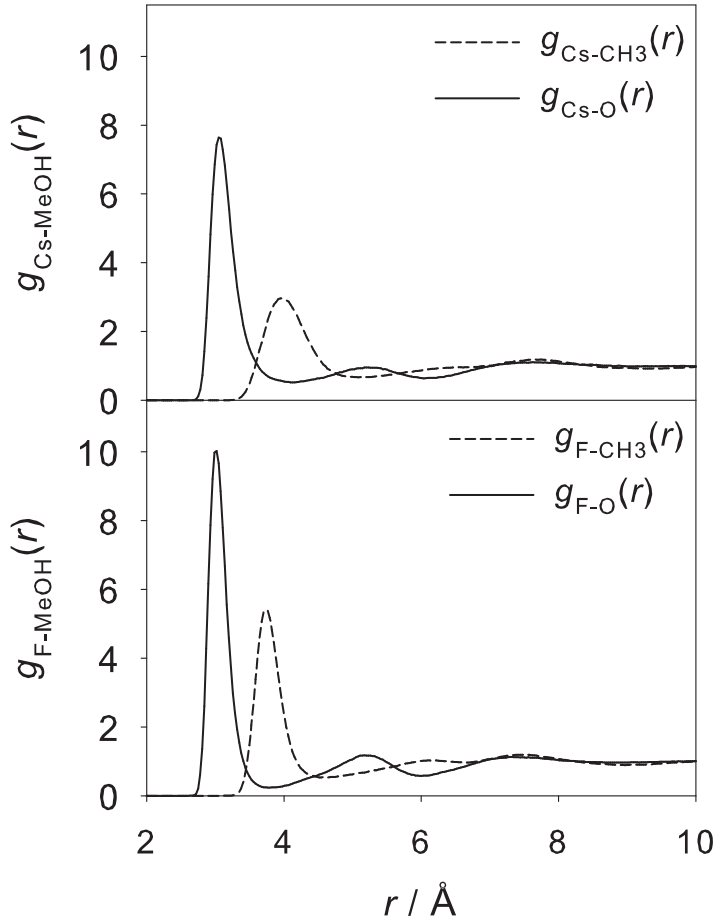

Figure 9: Position of the first maximum of the radial distribution function of the oxygen atom (top) and the methyl group (bottom) of methanol around the alkali cations (•) and halide anions (■) in methanolic solution (x_i=0.002 mol/mol) at 298.15 K and 1 bar. Present simulation data (filled symbols) are compared to experimental data from the literature (open symbols).[92,93] For lithium and sodium, the LJ size parameters are almost identical and the simulation results are identical within their statistical uncertainties. Experimental data are only available for the lithium cation.

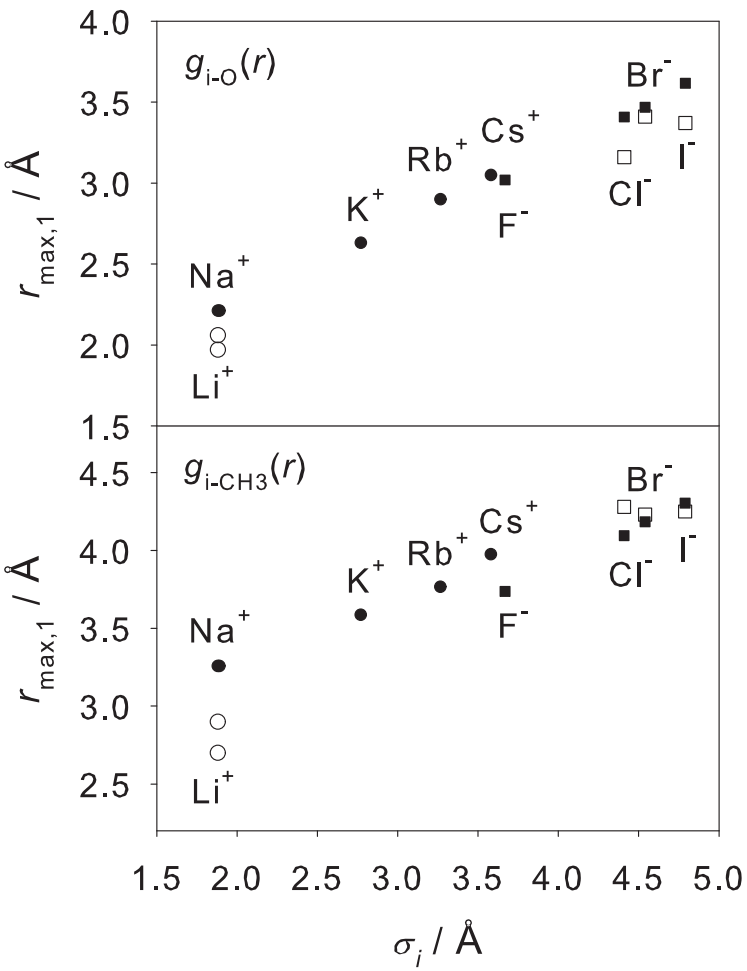

Figure 10: Solvation number of first solvation shell around the alkali cations (•) and halide anions (■) in methanolic solution (x_i=0.002 mol/mol) at 298.15 K and 1 bar. Present simulation data (filled symbols) are compared to experimental data from the literature (open symbols).[92,93] For lithium and sodium, the LJ size parameters and the simulation results are almost identical. Experimental data are only available for the lithium cation.

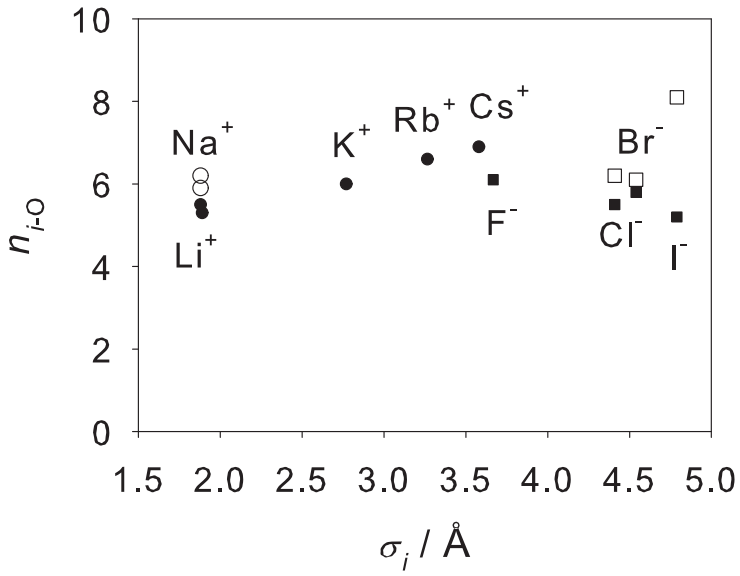

Figure 11: Self-diffusion coefficient of alkali cations (•) and halide anions (■) in methanolic solutions (x_i = 0.001 mol/mol) at 298.15 K and 1 bar. Present simulation data (filled symbols) are compared to experimental literature data (open symbols).[94] For lithium and sodium, the LJ size parameters are almost identical. Experimental data are only available for the sodium cation.

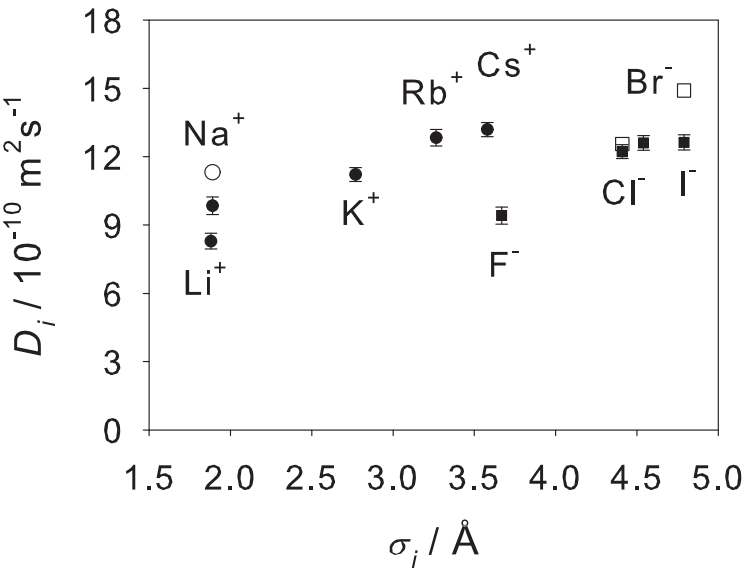

Figure 12: Electric conductivity of methanolic lithium, sodium and potassium chloride, bromide and iodide salt solutions as a function of the ion mole fraction at 298.15 K (except LiBr at 293.15 K) and 1 bar. Present simulation data (•) are compared to experimental data from the literature: Winsor and Cole[99] (∘), Bachhuber[100] (□), Sears et al.[95] (△), Foster and Amis[96] (▽), Kolthoff and Chantoon[97] (◇) and Goncharov et al.[98] (+).

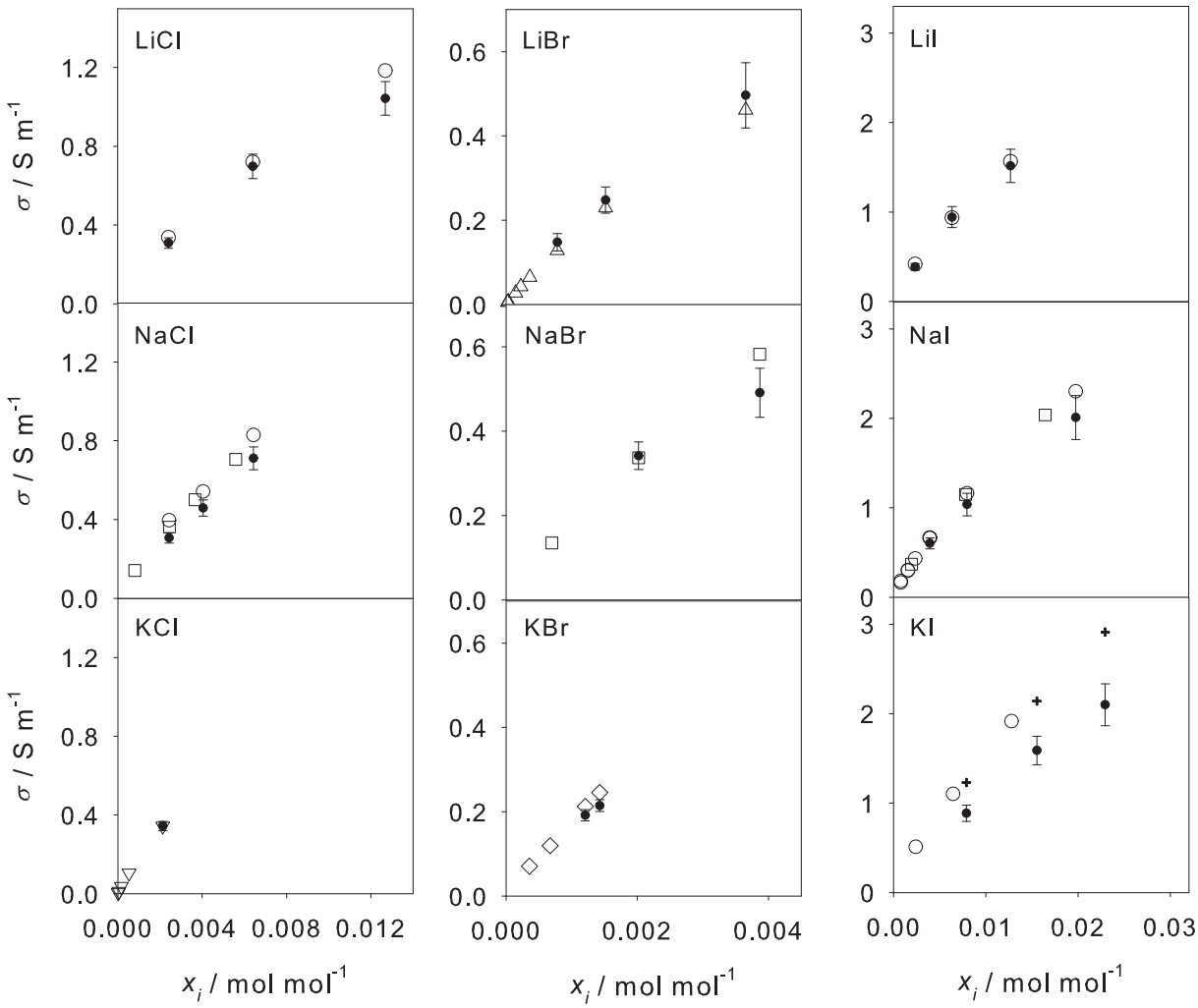

Table 1: Survey of experimental studies from the literature of the density ρ of methanolic alkali halide salt solutions at various temperature T and 1 bar.

	T / K		
salt	298.15	308.15	318.15
LiCl	47,51,53,54,57,59,63	59	59
LiBr	51,53,56–58,63	57	
LiI	56,57	57	
NaCl	52–54,58,59,65	59	59
NaBr	52,53,58,60,67	60,67	60
NaI	47,52,58,61,62	61,62	61
KF	52,53,58		
KCl	47,48,52,58,59	59	59
KBr	52,53,58,60,66	60	60
KI	47–50,52,53,58,61,62,64	49,61,62,64	49,61
RbCl	52		
RbBr	58		
RbI	58,62	62	
CsF	53,58		
CsCl	52,54		
CsBr	54,58		
CsI	52,55,62	62	

Table 2: Purity and supplier of the alkali halide salts.

salt	purity	supplier
LiCl	≥ 99 %	Merck
LiBr	≥ 99.999 %	Roth
LiI	≥ 99 %	AlfaAesar
NaCl	≥ 99.5 %	Merck
NaBr	≥ 99 %	Merck
NaI	≥ 99.5 %	Roth
KF	≥ 99 %	Merck
KCl	≥ 99.5 %	Merck
KBr	≥ 99.5 %	Merck
KI	≥ 99 %	Fluka
RbCl	≥ 99.8 %	Aldrich
RbBr	≥ 99.7 %	Aldrich
RbI	≥ 99.8 %	AlfaAesar
CsF	≥ 99.9 %	Aldrich
CsCl	≥ 99.999 %	Roth
CsBr	≥ 99.5 %	Fluka
CsI	≥ 99.999 %	Aldrich

Table 3: LJ size parameter σ, LJ energy parameter ε, point charge q and geometry parameters h and γ of the methanol force field, cf. Figure 2. The parameters were taken from previous work.[28]

site	σ_{aa} / Å	ε_{aa}/k_B / K	q_a / e
S_{CH3}	3.7543	120.592	+0.24746
S_{OH}	3.0300	87.879	−0.67874
S_H	0	0	+0.43128
	h_1 / Å	h_2 / Å	γ / °
	1.4246	0.9451	108.53

Table 4: LJ size parameter σ of alkali and halide ions. The LJ energy parameter ε/k_B is 200 K throughout. The parameters were taken from previous work.[20,22]

ion	σ / Å
Li^+	1.88
Na^+	1.89
K^+	2.77
Rb^+	3.26
Cs^+	3.58
F^-	3.66
Cl^-	4.41
Br^-	4.54
I^-	4.78

Table 5: Experimental data of the density ρ of methanolic alkali halide salt solutions and of pure methanol at various temperature T and 1 bar. The uncertainty in both the ion mole fraction x_i and the overall salt mole fraction x_S is estimated to be better than ±0.00001 mol/mol. The uncertainties of the density and temperature measurements are found to be better than ±0.0001 g/cm^3 and ±0.1 K, respectively.

T / K			298.15	308.15	318.15	T / K			298.15	308.15	318.15
salt	x_i/mol mol^{-1}	x_S/mol mol^{-1}	ρ / g cm^{-3}			salt	x_i/mol mol^{-1}	x_S/mol mol^{-1}	ρ / g cm^{-3}		
LiCl	0.0100	0.01010	0.7970	0.7879	0.7787	KBr	0.0012	0.00120	0.7898	0.7803	0.7708
	0.0200	0.02041	0.8073	0.7984	0.7895		0.0024	0.00241	0.7929	0.7835	0.7740
	0.0300	0.03093	0.8179	0.8093	0.8006		0.0036	0.00361	0.7960	0.7866	0.7771
	0.0400	0.04167	0.8280	0.8197	0.8112		0.0048	0.00482	0.7991	0.7897	0.7802
	0.0500	0.05263	0.8388	0.8306	0.8224	KI	0.0054	0.00543	0.8062	0.7967	0.7871
LiBr	0.0100	0.01010	0.8072	0.7979	0.7886		0.0108	0.01092	0.8258	0.8163	0.8067
	0.0200	0.02041	0.8279	0.8188	0.8096		0.0162	0.01647	0.8450	0.8355	0.8258
	0.0300	0.03093	0.8490	0.8400	0.8311		0.0216	0.02208	0.8646	0.8550	0.8453
	0.0400	0.04167	0.8707	0.8619	0.8531		0.0270	0.02775	0.8839	0.8744	0.8645
	0.0500	0.05263	0.8925	0.8839	0.8751	RbCl	0.0010	0.00100	0.7893	0.7799	0.7703
LiI	0.0100	0.01010	0.8168	0.8075	0.7980		0.0020	0.00200	0.7921	0.7826	0.7731
	0.0200	0.02041	0.8472	0.8379	0.8286		0.0030	0.00301	0.7946	0.7853	0.7757
	0.0300	0.03093	0.8785	0.8694	0.8601	RbBr	0.0011	0.00110	0.7906	0.7812	0.7717
	0.0400	0.04167	0.9097	0.9005	0.8914		0.0022	0.00220	0.7947	0.7853	0.7757
	0.0500	0.05263	0.9425	0.9334	0.9243		0.0033	0.00331	0.7987	0.7893	0.7797
NaCl	0.0017	0.00170	0.7891	0.7797	0.7701		0.0044	0.00442	0.8027	0.7933	0.7837
	0.0034	0.00341	0.7914	0.7821	0.7726	RbI	0.0026	0.00261	0.7987	0.7892	0.7796
	0.0051	0.00513	0.7940	0.7846	0.7752		0.0052	0.00523	0.8107	0.8012	0.7916
	0.0068	0.00685	0.7964	0.7871	0.7777		0.0078	0.00786	0.8227	0.8135	0.8038
NaBr	0.0080	0.00806	0.8060	0.7966	0.7871		0.0104	0.01051	0.8348	0.8251	0.8154
	0.0160	0.01626	0.8255	0.8162	0.8067		0.0130	0.01317	0.8467	0.8371	0.8273
	0.0240	0.02459	0.8449	0.8356	0.8261	CsF	0.0011	0.00110	0.7906	0.7812	0.7716
	0.0320	0.03306	0.8649	0.8556	0.8461		0.0022	0.00220	0.7946	0.7852	0.7756
	0.0400	0.04167	0.8850	0.8757	0.8663		0.0033	0.00331	0.7986	0.7892	0.7796
NaI	0.0100	0.01010	0.8203	0.8108	0.8012	CsCl	0.0012	0.00120	0.7910	0.7816	0.7720
	0.0200	0.02041	0.8546	0.8451	0.8355		0.0024	0.00241	0.7956	0.7862	0.7766
	0.0300	0.03093	0.8897	0.8801	0.8705		0.0036	0.00361	0.8001	0.7906	0.7810
	0.0400	0.04167	0.9246	0.9149	0.9051		0.0048	0.00482	0.8045	0.7950	0.7854
	0.0500	0.05263	0.9604	0.9506	0.9407	CsBr	0.0010	0.00100	0.7913	0.7818	0.7722
KF	0.0022	0.00220	0.7900	0.7806	0.7711		0.0020	0.00200	0.7961	0.7866	0.7770
	0.0044	0.00442	0.7933	0.7840	0.7745		0.0030	0.00301	0.8008	0.7913	0.7817
	0.0066	0.00664	0.7966	0.7873	0.7778	CsI	0.0010	0.00100	0.7923	0.7829	0.7733
	0.0088	0.00888	0.7998	0.7905	0.7811		0.0020	0.00200	0.7980	0.7885	0.7789
	0.0110	0.01112	0.8030	0.7938	0.7843		0.0030	0.00301	0.8037	0.7942	0.7846
KCl	0.0007	0.00070	0.7877	0.7783	0.7687		0.0040	0.00402	0.8094	0.7998	0.7902
	0.0014	0.00140	0.7889	0.7795	0.7699	MeOH			0.7865	0.7771	0.7675
	0.0021	0.00210	0.7900	0.7806	0.7711						

The composition is given in terms both of the ion mole fraction x_i and the overall salt mole fraction x_S. The ion mole fraction x_i is defined as $x_i = n_i/(2 \cdot n_i + n_{MeOH})$, where n_i is the mole number of each ion type and n_{MeOH} the mole number of methanol molecules in the electrolyte solution. For the 1:1 salt studied here, the ion mole fraction of the anions and the cations is x_i each. Regarding the salt as a single component, the salinity can also be quantified in terms the overall salt mole fraction x_S. It is defined as $x_S = n_S/(n_S + n_{MeOH})$, where n_S is the mole number of salt in the solution. The ion mole fraction x_i is related to the overall salt mole fraction x_S by $x_S = x_i/(1 - x_i)$ as the mole number of salt in the solution is $n_S = n_i$ here.

Table 6: Slope a of the density ρ of methanolic alkali halide salt solutions over the ion mole fraction x_i at various temperature T and 1 bar. For all lithium and sodium halide salts, the standard deviation $\Delta\rho$ of the correlation for the density of the methanolic electrolyte solutions, cf. Eq. (8), is smaller than ±0.001 g/cm^3. For the potassium, rubidium and cesium halides $\Delta\rho$ is even smaller than ±0.0002 g/cm^3.

T / K	298.15	318.15		298.15	318.15		298.15	318.15		298.15	318.15		298.15	318.15
salt	a / g cm^{-3}		Salt	a / g cm^{-3}		Salt	a / g cm^{-3}		Salt	a / g cm^{-3}		Salt	a / g cm^{-3}	
						KF	1.51	1.55				CsF	3.67	3.69
LiCl	1.04	1.10	NaCl	1.46	1.51	KCl	1.67	1.73	RbCl	2.73	2.77	CsCl	3.75	3.76
LiBr	2.10	2.14	NaBr	2.45	2.46	KBr	2.64	2.67	RbBr	3.70	3.71	CsBr	4.76	4.76
LiI	3.09	3.11	NaI	3.46	3.45	KI	3.61	3.60	RbI	4.64	4.62	CsI	5.72	5.50

Table 7: Molecular simulation data of the density ρ of methanolic alkali halide salt solutions over the ion mole fraction x_i and of pure methanol at various temperature T and 1 bar. The statistical uncertainties of the densities are throughout below ±0.0003 g/cm^3.

T / K		298.15	308.15	318.15
salt	x_i / mol mol^{-1}	ρ / g cm^{-3}		
LiCl	0.0100	0.7984	0.7892	0.7798
	0.0300	0.8164	0.8074	0.7998
	0.0500	0.8310	0.8244	0.8156
LiBr	0.0100	0.8085	0.7989	0.7889
	0.0300	0.8500	0.8409	0.8296
	0.0500	0.8851	0.8784	0.8678
LiI	0.0100	0.8195	0.8092	0.7991
	0.0300	0.8798	0.8701	0.8604
	0.0500	0.9402	0.9320	0.9228
NaCl	0.0034	0.7924	0.7830	0.7735
	0.0068	0.7972	0.7883	0.7791
NaBr	0.0080	0.8080	0.7988	0.7888
	0.0240	0.8481	0.8364	0.8279
	0.0400	0.8852	0.8767	0.8682
NaI	0.0100	0.8235	0.8131	0.8030
	0.0300	0.8922	0.8824	0.8725
	0.0500	0.9614	0.9530	0.9436
KF	0.0022	0.7918	0.7825	0.7717
	0.0066	0.7981	0.7891	0.7780
	0.0110	0.8054	0.7974	0.7858
KCl	0.0021	0.7915	0.7819	0.7720
KBr	0.0024	0.7936	0.7845	0.7742
	0.0048	0.7999	0.7906	0.7807
KI	0.0054	0.8065	0.7970	0.7877
	0.0162	0.8451	0.8360	0.8257
	0.0270	0.8817	0.8724	0.8618
RbCl	0.0030	0.7953	0.7854	0.7760
RbBr	0.0022	0.7954	0.7855	0.7763
	0.0044	0.8029	0.7938	0.7842
RbI	0.0026	0.7992	0.7901	0.7804
	0.0078	0.8217	0.8119	0.8037
	0.0130	0.8440	0.8355	0.8254
CsF	0.0033	0.8003	0.7902	0.7808
CsCl	0.0024	0.7961	0.7860	0.7771
	0.0048	0.8044	0.7947	0.7847
CsBr	0.0030	0.8006	0.7913	0.7815
CsI	0.0020	0.7985	0.7891	0.7791
	0.0040	0.8090	0.8001	0.7900
MeOH		0.7872	0.7778	0.7682

Table 8: RDF of the oxygen atom $g_{i-\mathrm{O}}(r)$ and methyl group $g_{i-\mathrm{CH3}}(r)$ of methanol around the alkali and halide ions i in methanolic solutions (x_i =0.002 mol/mol) at the first maximum $r_{\mathrm{max},1}$, first minimum $r_{\mathrm{min},1}$ and second maximum $r_{\mathrm{max},2}$ at 298.15 K and 1 bar.

	$r_{\mathrm{max},1}$ / Å		$g(r_{\mathrm{max},1})$	
ion	i-O	i-CH3	i-O	i-CH3
Li^+	2.212	3.258	21.77	5.848
Na^+	2.212	3.258	21.59	5.589
K^+	2.630	3.587	13.69	4.098
Rb^+	2.899	3.766	9.827	3.492
Cs^+	3.049	3.976	7.639	2.963
F^-	3.019	3.736	10.03	5.431
Cl^-	3.408	4.095	5.863	4.117
Br^-	3.467	4.185	5.206	3.893
I^-	3.617	4.304	4.190	3.620
	$r_{\mathrm{min},1}$ / Å		$g(r_{\mathrm{min},1})$	
ion	i-O	i-CH3	i-O	i-CH3
Li^+	3.258	4.005	0.049	0.135
Na^+	3.168	3.976	0.047	0.141
K^+	3.527	4.394	0.159	0.391
Rb^+	3.886	4.693	0.353	0.581
Cs^+	4.095	5.082	0.520	0.664
F^-	3.766	4.633	0.239	0.528
Cl^-	4.215	5.351	0.314	0.651
Br^-	4.304	5.500	0.410	0.666
I^-	4.394	5.799	0.349	0.671
	$r_{\mathrm{max},2}$ / Å		$g(r_{\mathrm{max},2})$	
ion	i-O	i-CH3	i-O	i-CH3
Li^+	4.394	5.410	1.605	1.234
Na^+	4.424	5.410	1.497	1.186
K^+	4.842	5.679	1.259	1.072
Rb^+	5.171	6.158	1.124	1.008
Cs^+	5.171	7.652	0.957	1.182
F^-	5.171	6.188	1.178	1.026
Cl^-	5.500	7.861	1.087	1.201
Br^-	5.440	7.921	1.068	1.187
I^-	5.530	8.011	1.155	1.200

Table 9: Solvation number $n_{i-\mathrm{O}}$ and residence time $\tau_{i-\mathrm{O}}$ of methanol molecules in the first solvation shell around the alkali and halide ions i in methanolic solutions (x_i = 0.002 mol/mol) and their self-diffusion coefficient D_i in methanolic solutions (x_i = 0.001 mol/mol) at 298.15 K and 1 bar. The number in parentheses indicates the statistical simulation uncertainty in the last digit.

ion	$n_{i-\mathrm{O}}$	$\tau_{i-\mathrm{O}}$ / ps	D_i / 10^{-10} $\mathrm{m^2s^{-1}}$
Li^+	5.5 (2)	66 (3)	8.3 (3)
Na^+	5.3 (2)	68 (3)	9.8 (4)
K^+	6.0 (2)	13 (1)	11.2 (3)
Rb^+	6.6 (2)	6.6 (4)	12.8 (4)
Cs^+	6.9 (2)	4.6 (3)	13.2 (3)
F^-	6.1 (2)	10 (1)	9.4 (4)
Cl^-	5.5 (2)	3.7 (3)	12.2 (3)
Br^-	5.8 (2)	4.6 (3)	12.6 (3)
I^-	5.2 (2)	2.8 (2)	12.6 (3)

References

(1) Barthel, J.; Gores, H. J.; Schmeer, G.; Wachter, R. Non-Aqueous Electrolyte-Solutions in Chemistry and Modern Technology. *Top. Curr. Chem.* **1983**, *111*, 33–144

(2) Gores, H. J.; Barthel, J. Non-Aqueous Eletrolyte-Solutions - Promising Materials for Electrochemical Technologies. *Naturwiss.* **1983**, *70*, 495–503

(3) Barthel, J. M. G.; Krienke, H.; Kunz, W. *Physical Chemistry of Electrolyte Solutions*; Springer, 1998

(4) Marcus, Y. On the molar volumes and viscosities of electrolytes. *J. Solution Chem.* **2006**, *35*, 1271–1286

(5) Horvath, A. L. *Handbook of Aqueous Electrolyte Solutions*; Ellis Horwood: Chichester, 1985

(6) Aqvist, J. Ion Water Interaction Potentials Derived From Free-energy Perturbation Simulations. *J. Phys. Chem.* **1990**, *94*, 8021–8024

(7) Dang, L. X. Fluoride-fluoride Association In Water From Molecular-dynamics Simulations. *Chem. Phys. Lett.* **1992**, *200*, 21–25

(8) Dang, L. X. Development of Nonadditive Intermolecular Potentials Using Molecular-dynamics - Solvation of Li+ and F- Ions In Polarizable Water. *J. Chem. Phys.* **1992**, *96*, 6970–6977

(9) Dang, L. X.; Garrett, B. C. Photoelectron-spectra of the Hydrated Iodine Anion From Molecular-dynamics Simulations. *J. Chem. Phys.* **1993**, *99*, 2972–2977

(10) Smith, D. E.; Dang, L. X. Computer-Simulations Of NaCl Association In Polarizable Water. *J. Chem. Phys.* **1994**, *100*, 3757–3766

(11) Dang, L. X. Mechanism and Thermodynamics of Ion Selectivity In Aqueous-solutions of 18-crown-6 Ether - A Molecular-dynamics Study. *J. Am. Chem. Soc.* **1995**, *117*, 6954–6960

(12) Peng, Z. W.; Ewig, C. S.; Hwang, M. J.; Waldman, M.; Hagler, A. T. Derivation of class II force fields. 4. van der Waals parameters of alkali metal cations and halide anions. *J. Phys. Chem. A* **1997**, *101*, 7243–7252

(13) Wheeler, D. R.; Newman, J. Molecular dynamics simulations of multicomponent diffusion. 1. Equilibrium method. *J. Phys. Chem. B* **2004**, *108*, 18353–18361

(14) Jensen, K. P.; Jorgensen, W. L. Halide, ammonium, and alkali metal ion parameters for modeling aqueous solutions. *J. Chem. Theory Comput.* **2006**, *2*, 1499–1509

(15) Joung, I. S.; Cheatham, T. E. Determination of alkali and halide monovalent ion parameters for use in explicitly solvated biomolecular simulations. *J. Phys. Chem. B* **2008**, *112*, 9020–9041

(16) Horinek, D.; Mamatkulov, S. I.; Netz, R. R. Rational design of ion force fields based on thermodynamic solvation properties. *J. Chem. Phys.* **2009**, *130*, 124507

(17) Klasczyk, B.; Knecht, V. Kirkwood-Buff derived force field for alkali chlorides in simple point charge water. *J. Chem. Phys.* **2010**, *132*, 024109

(18) Reif, M. M.; Hünenberger, P. H. Computation of methodology-independent single-ion solvation properties from molecular simulations. IV. Optimized Lennard-Jones interaction parameter sets for the alkali and halide ions in water. *J. Chem. Phys.* **2011**, *134*, 144104

(19) Gee, M. B.; Cox, N. R.; Jiao, Y. F.; Bentenitis, N.; Weerasinghe, S.; Smith, P. E. A Kirkwood-Buff Derived Force Field for Aqueous Alkali Halides. *J. Chem. Theory Comput.* **2011**, *7*, 1369–1380

(20) Reiser, S.; Deublein, S.; Vrabec, J.; Hasse, H. Molecular dispersion energy parameters for alkali and halide ions in aqueous solution. *J. Chem. Phys.* **2014**, *140*, 044504

(21) Moucka, F.; Nezbeda, I.; Smith, W. R. Molecular force fields for aqueous electrolytes:

SPC/E-compatible charged LJ sphere models and their limitations. *J. Chem. Phys.* **2013**, *138*, 154102

(22) Deublein, S.; Vrabec, J.; Hasse, H. A set of molecular models for alkali and halide ions in aqueous solution. *J. Chem. Phys.* **2012**, *136*, 084501

(23) Reiser, S.; Horsch, M.; Hasse, H. Temperature Dependence of the Density of Aqueous Alkali Halide Salt Solutions by Experiment and Molecular Simulation. *J. Chem. Eng. Data* **2014**, *59*, 3434–3448

(24) Gonzalez-Salgado, D.; Dopazo-Paz, A.; Gomez-Alvarez, P.; Miguez, J. M.; Vega, C. Solid-Solid and Solid-Fluid Equilibria of the Most Popular Models of Methanol Obtained by Computer Simulation. *J. Phys. Chem. B* **2011**, *115*, 3522–3530

(25) Jorgensen, W. L. Optimized Intermolecular Potential Functions for Liquid Alcohols. *J. Phys. Chem.* **1986**, *90*, 1276–1284

(26) Haughney, M.; Ferrario, M.; McDonald, I. R. Molecular-Dynamics Simulation of Liquid Methanol. *J. Phys. Chem.* **1987**, *91*, 4934–4940

(27) Van Leeuwen, M. E.; Smit, B. Molecular Simulation of the Vapor-Liquid Coexistence Curve of Methanol. *J. Phys. Chem.* **1995**, *99*, 1831–1833

(28) Schnabel, T.; Srivastava, A.; Vrabec, J.; Hasse, H. Hydrogen bonding of methanol in supercritical CO2: Comparison between H-1 NMR spectroscopic data and molecular simulation results. *J. Phys. Chem. B* **2007**, *111*, 9871–9878

(29) Guevara-Carrion, G.; Nieto-Draghi, C.; Vrabec, J.; Hasse, H. Prediction of Transport Properties by Molecular Simulation: Methanol and Ethanol and Their Mixture. *J. Phys. Chem. B* **2008**, *112*, 16664–16674

(30) de Reuck, K. M.; Craven, R. J. B. In *Methanol, International Thermodynamic Tables of the Fluid State - 12*; Blackwell Scientific Publications, London, 1993

(31) Impey, R. W.; Spirk, M.; Klein, M. L. Ionic Solvation in Nonaqueous Solvents - the Structure of Li+ and Cl- in Methanol, Ammonia and Methylamine. *J. Am. Chem. Soc.* **1987**, *109*, 5900–5904

(32) Marx, D.; Heinzinger, K.; Palinkas, I., G. Bako Structure and Dynamics of NaCl in Methanol - A Molecular-Dynamics Study. *Z. Naturforsch. A-A J. Phys. Sci.* **1991**, *46*, 887–897

(33) Sese, G.; Guardia, E.; Padro, J. Molecular Dynamics Study of Na+ and Cl- in Methanol. *J. Chem. Phys.* **1996**, *105*, 8826–8834

(34) Sese, G.; Padro, J. A. Solvation dynamics: The role of hydrogen bonding. *J. Chem. Phys.* **1998**, *108*, 6347–6352

(35) Hawlicka, E.; Swiatla-Wojcik, D. Dynamic Properties of the NaCl-Methanol-Water Systems - MD Simulation Studies. *Phys. Chem. Chem. Phys.* **2000**, *2*, 3175–3180

(36) Kim, H. S. Solvent Effect on K+ to Na+ Ion Mutation: A Monte Carlo Simulation Study. *J. Mol. Struct.: THEOCHEM* **2001**, *540*, 79–89

(37) Hawlicka, E.; Swiatla-Wojcik, D. Effect of sodium halides on the structure of methanol-water mixture - MD simulation studies. *J. Mol. Liq.* **2002**, *98-99*, 355–365

(38) Hawlicka, E.; Swiatla-Wojcik, D. MD Simulation Studies of Selective Solvation in Methanol-Water Mixtures: An Effect of the Charge Density of a Solute. *J. Phys. Chem. A* **2002**, *106*, 1336–1345

(39) Hawlicka, E.; Swiatla-Wojcik, D. Aggregation of ions in methanol-water solutions of sodium halides. *J. Chem. Phys.* **2003**, *119*, 2206–2213

(40) Pagliai, M.; Cardini, G.; Schettino, V. Solvation Dynamics of Li+ and Cl- Ions in Liquid Methanol. *J. Phys. Chem. B* **2005**, *109*, 7475–7481

(41) Chowdhuri, S.; Chandra, A. Solute size effects on the solvation structure and diffusion of ions in liquid methanol under normal and cold condition. *J. Chem. Phys.* **2006**, *124*, 084507

(42) Faralli, C.; Pagliai, M.; Cardini, G.; Schettino, V. Structure and dynamics of Br- ion in liquid methanol. *J. Phys. Chem. B* **2006**, *110*, 14923–14928

(43) Faralli, C.; Pagliai, M.; Cardini, G.; Schettino, V. The Solvation Dynamics of Na+ and K+ Ions in Liquid Methanol. *Theor. Chem. Acc.* **2007**, *118*, 417–423

(44) Wang, L., Ed. *Molecular Dynamics - Theoretical Developments and Applications in Nanotechnology and Energy*; InTech: Rijeka, 2012

(45) Chowdhuri, S.; Pattanayak, S. K. Pressure effects on the dynamics of ions and solvent molecules in liquid methanol under ambient and cold conditions: Importance of solvent's H-bonding network. *J. Mol. Liq.* **2013**, *180*, 172–178

(46) Kumar, P.; Varanasi, S. R.; Yashonath, S. Relation Between the Diffusivity, Viscosity, and Ionic Radius of LiCl in Water, Methanol, and Ethylene Glycol: A Molecular Dynamics Simulation. *J. Phys. Chem. B* **2013**, *117*, 8196–8208

(47) Vosburgh, W.; Connell, L.; Butler, J. The Electrostriction Produced by Salts in some Aliphatic Alcohols. *J. Chem. Soc.* **1933**, 933–942

(48) Jones, G.; Fornwalt, H. J. The viscosity of solutions of salts in methanol. *J. Am. Chem. Soc.* **1935**, *57*, 2041–2045

(49) Briscoe, H. T.; Rinehart, W. T. Studies of Relative Viscosity of Non-Aqueous Solutions. *J. Phys. Chem.* **1942**, *46*, 387–394

(50) MacInnes, D. A.; Dayhoff, M. O. The Apperent and Partial Molal Volumes of Potassium Iodide and of Iodine in Methanol at 25ÂřC from Density Measurements. *J. Am. Chem. Soc.* **1953**, *75*, 5219–5220

(51) Skabichevskii, P. A. Apprarent Molar Volumes of Lithium Salts in Methyl and Isopentyl Alcohol. *Russ. J. Phys. Chem.* **1972**, *46*, 309–310

(52) Kawaizumi, F.; Zana, R. Partial Molal Volumes of Ions in Organic Solvents from Ultrasonic Vibration Potential and Density Measurements. 1. Methanol. *J. Phys. Chem.* **1974**, *78*, 627–634

(53) Pasztor, A. J.; Criss, C. M. Apparent Molal Volumes adn Heat Capacities of Some 1-1 Electrolytes in Anhydrous Methanol at 25ÂřC. *J. Sol. Chem.* **1978**, *7*, 27–44

(54) Werblan, L. Viscous-Flow Mechanism in Water-Methanol Solutions of Alkali-Metal Halides. 1. *B. Acad. Pol. Sci. Chim.* **1979**, *27*, 873–890

(55) Werblan, L. Viscous-Flow Mechanism in Water-Alcohol Solutions of Cesium Iodide. 2. *B. Acad. Pol. Sci. Chim.* **1979**, *27*, 903–917

(56) Renz, M. Bestimmung thermodynamischer Eigenschaften waessriger und methylalkoholischer Salzloesungen. Ph.D. thesis, University of Essen, 1981

(57) Glugla, P. G.; Byon, J. H.; Eckert, C. A. Partial Molar Volume of Some Monovalent Salts and Polar Molecules in Organic Solvents. *J. Chem. Eng. Data* **1982**, *27*, 393–398

(58) Lankford, J. I.; Holladay, W. T.; Criss, C. M. Isentropic Compressibilities of Univalent Electrolytes in Methanol at 25ÂřC. *J. Sol. Chem.* **1984**, *13*, 699–720

(59) Takenaka, N.; Takemura, T.; Sakurai, M. Partial Molal Volumes of Uni-Univalent Electrolytes in Methanol Plus Water. 1. Lithium-Chloride, Sodium-Chloride, and Potassium-Chloride. *J. Chem. Eng. Data* **1994**, *39*, 207–213

(60) Takenaka, N.; Takemura, T.; Sakurai, M. Partial Molal Volumes of Uni-Univalent Electrolytes in Methanol Plus Water. 2. Sodium-Bromide, and Potassium-Bromide. *J. Chem. Eng. Data* **1994**, *39*, 796–801

(61) Takenaka, N.; Takemura, T.; Sakurai, M. Partial Molal Volumes of Uni-Univalent Electrolytes in Methanol Plus Water. 3. Sodium-Iodide and Potassium-Iodide. *J. Chem. Eng. Data* **1994**, *39*, 802–807

(62) Figurski, G.; Nipprasch, D. Densities of concentrated solutions of NaI, KI, RbI, or CsI in methanol at temperatures from 298.15 K to 313.15 K. *ELDATA: Int. Electron. J. Phys.-Chem. Data* **1996**, *199*, 149–152

(63) Kiepe, J.; Rodrigues, A.; Horstmann, S.; Gmehling, J. Experimental Determination and Correlation of Liquid Density Data of Electrolyte Mixtures Containing Water or Methanol. *Ind. Eng. Chem. Res.* **2003**, *42*, 2022–2029

(64) Gonzalez, B.; Dominguez, A.; Tojo, J.; Esteves, M.; Cardoso, A.; Barcia, O. Dynamic Viscosities of KI or NH4I in Methanol and NH4I in Ethanol at Several Temperatures and 0.1 MPa. *J. Chem. Eng. Data* **2005**, *50*, 109–112

(65) Eliseeva, O. V.; Golubev, V. V.; Dyshin, A. A.; Kiselev, M. G.; Al'per, G. A. A volumetric investigation of solvophobic effects in halide-n-alkanol-n-alkane ternary systems. *Russ. J. Phys. Chem.* **2006**, *80*, 205–209

(66) Kolhapurkar, R. R.; Patil, P. K.; Dagade, D. H.; Patil, K. J. Studies of Thermodynamic Properties of Binary and Ternary Methanolic Solutions Containing KBr and 18-Crown-6 at 298.15 K. *J. Sol. Chem.* **2006**, *35*, 1357–1376

(67) Wawer, J.; Krakowiak, J.; Grzybkowski, W. Apparent molar volumes, expansibilities, and isentropic compressibilities of selected electrolytes in methanol. *J. Chem. Thermodyn.* **2008**, *40*, 1193–1199

(68) Turner, W.; Bissett, C. The solubilities of alkali haloids in methyl, ethyl, propyl, and isoamyl alcohols. *J. Chem. Soc.* **1913**, *103*, 1904–1910

(69) Meyer, K. H.; Dunkel, M. *Bronstein-Festband, Akademische Verlags Gesellschaft, Leipzig* **1931**, 553–573

(70) Akerlof, G.; Turck, H. The solubility of some strong, highly soluble electrolytes in methyl

alcohol and hydrogen peroxide-water mixtures at 25ÂřC. *J. Am. Chem. Soc.* **1935**, *57*, 1746–1750

(71) Pavlopoulos, T.; Strehlow, H. Die Löslichkeit der Alkalihalogenide in Methylalkohol, Acetonitril und Ameisensäure. *Z. Phys. Chem. (Leipzig, Germany)* **1954**, *202*, 474

(72) Harner, R. E.; Sydnor, J. B.; S., G. E. Solubilites of Anhydrous Ionic Substance in Absolute Methanol. *J. Chem. Eng. Data* **1963**, *8*, 411–412

(73) Emons, H.; Winkler, F. Über das Verhalten der Alkalihalogenide in Methanol-Wasser-Mischungen. *Z. Chem.* **1971**, *11*, 293–304

(74) Vlasov, Y. G.; Antonov, P. P. NaCl-NaBr-H2O and NaCl-NaBr-CH3OH Systems at 25 Degrees C. *Russ. J. Inorg. Chem.* **1971**, *16*, 115–117

(75) Kovalenko, L. S.; Ivanova, E. F.; Krasnoperova, A. P. Study of Sodium-Chloride Dissolution Thermodynamics in the Acetonitril-Methanol System. *Russ. J. Phys. Chem.* **1983**, *57*, 1790–1792

(76) Pinho, S. P.; Macedo, E. A. Representation of salt solubility in mixed solvents: A comparison of thermodynamic models. *Fluid Phase Equilib.* **1996**, *116*, 209–216

(77) Wagner, K.; Friese, T.; Schulz, S.; Ulbig, P. Solubilities of sodium chloride in organic and aqueous-organic solvent mixtures. *J. Chem. Eng. Data* **1998**, *43*, 871–875

(78) Li, M.; Constantinescu, D.; Wang, L.; Mohs, A.; Gmehling, J. Solubilities of NaCl, KCl, LiCl, and LiBr in Methanol, Ethanol, Acetone, and Mixed Solvents and Correlation Using the LIQUAC Model. *Ind. Eng. Chem. Res.* **2010**, *49*, 4981–4988

(79) Li, M.-Y.; Wang, L.-S.; Wang, K.-P.; Jiang, B.; Gmehling, J. Experimental measurement and modeling of solubility of LiBr and LiNO3 in methanol, ethanol, 1-propanol, 2-propanol and 1-butanol. *Fluid Phase Equilib.* **2011**, *307*, 104–109

(80) Lorentz, H. Über die Anwendung des Satzes vom Virial in der kinetischen Theorie der Gase. *Ann. Phys.* **1881**, *248*, 127–136

(81) Berthelot, D. Sur le melange des gaz. *C. R. Acad. Sci.* **1898**, *126*, 1703–1706

(82) Allen, M.; Tildesley, D. *Computer Simulation of Liquids*; Clarendon Press: Oxford, 1987

(83) Robinson, R. A.; Stokes, R. H. *Electrolyte Solutions*, 2nd ed.; Butterworth: London, 1955

(84) Koneshan, S.; Rasaiah, J. C.; Lynden-Bell, R. M.; Lee, S. H. Solvent structure, dynamics, and ion mobility in aqueous solutions at 25 degrees C. *J. Phys. Chem. B* **1998**, *102*, 4193–4204

(85) Impey, R. W.; Madden, P. A.; McDonald, I. R. Hydration And Mobility of Ions in Solution. *J. Phys. Chem.* **1983**, *87*, 5071–5083

(86) Green, M. Markoff Random Processes and the Statistical Mechanics of Time-Dependent Phenomena.2. Irreversible Processes in Fluids. *J. Chem. Phys.* **1954**, *22*, 398–413

(87) Kubo, R. Statistical-Mechanical Theory of Irreversible Processes. 1. General Theory and Simple Applications to Magnetic and Conduction Problems. *J. Phys. Soc. Jpn.* **1957**, *12*, 570–586

(88) Gubbins, K. *Statistical Mechanics Vol. 1*; The Chemical Society Burlington House: London, 1972

(89) Hansen, J. P.; McDonald, I. *Theory of Simple Liquids*; Academic Press: Amsterdam, 1986

(90) Glass, C. W.; Reiser, S.; Rutkai, G.; Deublein, S.; Koester, A.; Guevara-Carrion, A., G. Wafai; Horsch, M.; Bernreuther, M.; Windmann, T.; Hasse, H.; Vrabec, J. ms2: A molecular simulation tool for thermodynamic properties, new version release. *Comput. Phys. Commun.* **2014**, *185*, 3302–3306

(91) Smirnov, P. R. Comparative Review of Structural Parameters of the Nearest Surrounding of Monoatomic Cations in Water and Methanol Media. *Russ. J. Gen. Chem.* **2013**, *83*, 1967–1975

(92) D' Angelo, P.; Di Nola, A.; Mangoni, M.; Pavel, N. V. An extended X-ray absorption fine structure study by employing molecular dynamics simulations: Bromide ion in methanolic solution. *J. Chem. Phys.* **1996**, *104*, 1779–1790

(93) Megyes, T.; Radnai, T.; Grosz, T.; Palinkas, G. X-ray diffraction study of lithium halides in methanol. *J. Mol. Liq.* **2002**, *101*, 3–18,

(94) Hawlicka, E. Self-Diffusion of Sodium, Chloride and Iodide-Ions in Methanol-Water Mixture. *Z. Naturforsch. A-A J. Phys. Sci.* **1986**, *41*, 939–943

(95) Sears, P. G.; McNeer, R. L.; Dawson, L. R. Conductance of Lithium Bromide at Low Concentrations in Methanol within the Tempe Range 20-Degrees to 50-Degrees. *J. Electrochem. Soc.* **1955**, *102*, 269–271

(96) Foster, N. G.; Amis, E. The Equivalent Conductance of Electrolytes in Mixed Solvents. I. Potassium Chloride in the Water - Methanol System. *Z. Phys. Chem.* **1955**, *3*, 365–381

(97) Kolthoff, I. M.; Chantoon, M. K. Critical Study Involving Water, Methanol, Acetonitrile, N,N-Dimethylformamide, and Dimethyl Sulfoxide of Medium Ion Activity Coefficients γ on the Basis of the γ_{AsPh4+}=γ_{BPh4-} Assumption. *J. Phys. Chem.* **1972**, *76*, 2024–2034

(98) Goncharov, V. S.; Yastremskii, P. S.; Lyashchenko, A. K. Electric Conductivity of Electrolyte Solutions in Temperature Dependence and its Relation to the Structure of the Aqueous Solvent. *Russ. J. Phys. Chem.* **1981**, *55*, 1020–1023

(99) Winsor, P.; Cole, R. H. Dielectric Properties of Electrolyte Solutions. 2. Alkali-Halides in Methanol. *J. Phys. Chem.* **1982**, *86*, 2491–2494

(100) Bachhuber, K. The Influence of Electrolytes on Structural and Dynamic Properties of Methanol, N,N-Dimethylformamide, N-Methylformamide and Formamide. Ph.D. thesis, University of Regensburg, 1989

(101) Flyvbjerg, H.; Petersen, H. G. Error-Estimates On Averages of Correlated Data. *J. Chem. Phys.* **1989**, *91*, 461–466

(102) Ewald, P. P. Die Berechnung optischer und elektrostatischer Gitterpotenziale. *Ann. Phys.* **1921**, *369*, 253–287

(103) Guevara-Carrion, G.; Vrabec, J.; Hasse, H. Prediction of self-diffusion coefficient and shear viscosity of water and its binary mixtures with methanol and ethanol by molecular simulation. *J. Chem. Phys.* **2011**, *134*, 074508

For Table of Contents Only

Title: Density of methanolic alkali halide salt solutions by experiment and molecular simulation

Authors: S. Reiser, M. Horsch, H. Hasse